MOLECULAR AND CELLULAR BIOLOGY, June 2005, p. 4767–4781 Vol. 25, No. 11
0270-7306/05/$08.00+0 doi:10.1128/MCB.25.11.4767–4781.2005

Novel Response to Microtubule Perturbation in Meiosis†

Andreas Hochwagen,[1] Gunnar Wrobel,[2] Marie Cartron,[2] Philippe Demougin,[2] Christa Niederhauser-Wiederkehr,[2] Monica G. Boselli,[1] Michael Primig,[2]‡ and Angelika Amon[1]‡*

Center for Cancer Research, Howard Hughes Medical Institute, Massachusetts Institute of Technology, E17-233, 40 Ames St., Cambridge, Massachusetts 02139,[1] and Biozentrum & Swiss Institute of Bioinformatics, Klingelbergstrasse 50-70, CH-4056 Basel, Switzerland[2]

Received 7 December 2004/Returned for modification 19 January 2005/Accepted 24 February 2005

During the mitotic cell cycle, microtubule depolymerization leads to a cell cycle arrest in metaphase, due to activation of the spindle checkpoint. Here, we show that under microtubule-destabilizing conditions, such as low temperature or the presence of the spindle-depolymerizing drug benomyl, meiotic budding yeast cells arrest in G_1 or G_2, instead of metaphase. Cells arrest in G_1 if microtubule perturbation occurs as they enter the meiotic cell cycle and in G_2 if cells are already undergoing premeiotic S phase. Concomitantly, cells down-regulate genes required for cell cycle progression, meiotic differentiation, and spore formation in a highly coordinated manner. Decreased expression of these genes is likely to be responsible for halting both cell cycle progression and meiotic development. Our results point towards the existence of a novel surveillance mechanism of microtubule integrity that may be particularly important during specialized cell cycles when coordination of cell cycle progression with a developmental program is necessary.

In the course of gamete production, a specialized cell division called meiosis creates four haploid cells from one diploid progenitor. Many aspects of cell cycle regulation are similar during proliferative mitotic growth and meiosis, but the different division pattern of meiosis requires modification of the mitotic cell cycle machinery to fit the needs of the meiotic differentiation program. During the meiotic cell cycle, DNA is replicated once and then separated twice during meiosis I and meiosis II without an intervening S phase. In addition, a prolonged G_2 phase (meiotic prophase) separates premeiotic DNA replication from the first meiotic division. During meiotic prophase, homologous chromosomes align, and meiotic recombination creates the links between homologs that are necessary for proper meiosis I chromosome segregation. After completion of prophase, homologous chromosomes are segregated first during meiosis I, followed by the segregation of sister chromatids during meiosis II.

Concurrent with the chromosomal events, cells progress through an intricate developmental program that culminates in the production of highly specialized cell types, such as sperm and egg, or spores in budding yeast. For gamete formation to occur successfully, it is essential that the meiotic cell cycle and the developmental program are tightly coupled via molecular interactions that we are only beginning to understand. Mutations that uncouple meiotic cell cycle progression from spore formation emphasize how important these interactions are. For example, cells that fail to decrease cyclin-dependent kinase (CDK) activity cannot disassemble the meiosis I spindle, but other aspects of the meiotic cell cycle and the developmental program (spore production) continue, leading to the formation of defective gametes (5, 36).

The complex transcriptional program that underlies gametogenesis appears to be one key level of control that couples the meiotic cell cycle to gamete development. Stage-specific expression of crucial meiotic regulators controls most meiotic processes, including meiotic recombination, formation of the synaptonemal complex (SC), meiosis I chromosome segregation, and spore wall formation. Factors required for the respective cell cycle stage and the corresponding developmental genes are coordinately up-regulated within characteristic transcriptional waves, creating a link between cell cycle and development (7, 8, 44). For example, nutrient limitation that provides the signal for entry into the meiotic cell cycle is relayed through the transcription factor Ime1 (17), which is not only essential for initiating cell cycle entry but also responsible for inducing the transcription of genes required for the early metabolic program of gametogenesis. It does so by interacting with the transcriptional modulator Ume6 that coordinates expression of at least 80 loci involved in metabolic, as well as early and middle meiotic, gene functions (68). Similarly, at the end of meiotic prophase, the transcription factor Ndt80 induces not only expression of genes essential for entry into meiosis I but also that of genes important for prospore wall assembly (7, 8, 44).

Several meiotic events are monitored by surveillance mechanisms known as checkpoints. Checkpoints halt cell cycle progression until the event that is surveyed has been completed, thereby ensuring that the cell cycle, as well as developmental events, occur in an ordered manner. Typically, the transcription factors required to initiate the next phase of the meiotic cell cycle are under direct checkpoint control. For example, the transcription factor *NDT80* is a direct target of the recombination (or pachytene) checkpoint (49, 63), which prevents entry into meiosis I and prospore wall assembly until the DNA

* Corresponding author. Mailing address: Center for Cancer Research, Howard Hughes Medical Institute, Massachusetts Institute of Technology, E17-233, 40 Ames St., Cambridge MA 02139. Phone: (617) 258-8964. Fax: (617) 258-6558. E-mail: angelika@mit.edu.

† Supplemental material for this article may be found at http://mcb.asm.org/.

‡ M.P. and A.A. made an equal contribution.

TABLE 1. Strains

Strain	Relevant genotype
A727	*MAT***a**/α *ho*::*LYS2*/*ho*::*LYS2 lys2*/*lys2 his4X*/*his4X leu2*::*hisG*/*leu2*::*hisG ura3*/*ura3*
A1771	*MAT***a**/α *rad50*::*URA3*/*rad50*::*URA3*
A1972	*MAT***a**/α *REC8-3HA*::*URA3*/*REC8-3HA*::*URA3*
A4563	*MAT***a**/α *CLB3-3HA*::*kanMX6*/+
A4704	*MAT***a**/α *swe1*Δ::*kanMX4*/*swe1*Δ::*kanMX4, CLB3-3HA*::*kanMX6*/+
A4838	*MAT***a**/α *mek1*Δ::*kanMX4*/*mek1*Δ::*kanMX4*
A4843	*MAT***a**/α *mad2*::*kanMX*/*mad2*::*kanMX, CLB3-3HA*::*kanMX6*/+
A4967	*MAT***a**/α *URA3*::*tetOx224* (Chr.V)/+ *LEU2*::*pURA3-tetR-GFP*/*LEU2*::*pURA3-tetR-GFP*::*tetO*::*HIS3* (*Chr.III*)
A5009	*MAT***a**/α *URA3*::*tetOx224* (Chr.V)/*URA3*::*tetOx224* (Chr.V) *LEU2*::*pURA3*::*tetR-GFP*/*LEU2*::*pURA3*:: *tetR-GFP*
A5779	*MAT***a**/α *tub2-150*/*tub2-150 CLB3-3HA*::*kanMX6*/+
A12927	*MAT***a**/α *mad2*::*kanMX*/*mad2*::*kanMX mek1*Δ::*kanMX4*/*mek1*Δ::*kanMX4 CLB3-3HA*::*kanMX6*/+

damage created during meiotic recombination is repaired. Thus, both the initiation of prospore wall assembly and entry into meiosis I are coupled to the completion of meiotic prophase.

The integrity of the microtubule cytoskeleton is also monitored by surveillance mechanisms. In mitotic cells, perturbations of the microtubule cytoskeleton lead to unattached kinetochores, which cause activation of the spindle assembly checkpoint (32, 56, 57). The spindle checkpoint component Mad2 binds to and inhibits the anaphase-promoting complex or cyclosome (APC/C), a crucial activator of chromosome segregation (20). This inhibition causes a cell cycle arrest in metaphase until the spindle defects have been repaired. Disruption of the microtubule cytoskeleton during the meiotic cell cycle by exposure to the microtubule-depolymerizing drug benomyl (methyl 1-[butylcarbamoyl]-2-benzimidazolecarbamate) has also been reported to cause a transient delay in metaphase I that, much like in the mitotic cell cycle, is dependent upon the checkpoint component Mad2 (56).

Here, we report that severe disruption of the yeast microtubule cytoskeleton after premeiotic DNA replication leads to a G_2 rather than a metaphase I arrest, with low protein levels of cyclin Clb3 and incompletely synapsed chromosomes. Whole-genome expression profiling revealed that this arrest is accompanied by a substantial change in the meiotic gene expression program. In particular, genes essential for meiotic recombination, cell cycle progression, or spore formation and/or maturation are not expressed at wild-type levels. Down-regulation of meiotic transcripts also occurs when microtubules are destabilized by culturing cells at 10°C. Finally, we demonstrate that the G_2 arrest caused by microtubule depolymerization is independent of the checkpoints controlling spindle assembly and meiotic recombination. Our results indicate that the transcriptional response to microtubule perturbations serves to bring both the meiotic developmental program and the cell cycle to a halt. Our data also point towards the existence of a novel mechanism of microtubule integrity surveillance that coordinates the meiotic cell cycle with spore development.

MATERIALS AND METHODS

Strains. Strains used are described in Table 1 and are derivatives of SK1 (24). *CLB3-3HA*::*kanMX6* and *mad2*Δ::*kanMX6* were constructed by a one-step gene replacement method (34). *mek1*::*kanMX4* and *swe1*::*kanMX4* were PCR amplified from the corresponding knockout strains in the *Saccharomyces* deletion collection (13) and introduced into SK1. *REC8-3HA* and *URA3*::*tetO* were described in reference 27 and *LEU2*::*pURA3-tetR-GFP*::*tetO*::*HIS3* was described in reference 37. *rad50*::*URA3* was described in reference 6.

Sporulation conditions. Cells were grown to saturation in YPD (yeast extract-peptone plus 2% glucose) for 24 h, diluted into YPA (yeast extract-peptone plus 2% potassium acetate) at an optical density at 600 nm of 0.3 and grown overnight (16 h) at 30°C. Cells were washed with sterilized water the next day and resuspended in SPO medium (0.3% potassium acetate; pH = 7.0) at an optical density at 600 nm of 1.9 to induce sporulation. Cells were sporulated at 25°C or 10°C as indicated. Sporulation medium containing benomyl was always prepared freshly on the day of the experiment, following the directions in reference 56. Briefly, dimethyl sulfoxide (DMSO; Sigma-Aldrich) or benomyl (30 mg/ml stock in DMSO; Sigma-Aldrich) was dissolved in near-boiling SPO medium to avoid precipitation of benomyl. The medium was then allowed to slowly cool to room temperature. At the time of drug treatment, cells were filtered and immediately resuspended in the medium containing benomyl or DMSO.

Immunofluorescence and meiotic spreads. Unless noted otherwise, 200 cells were scored for each time point. Indirect immunofluorescence on whole cells was carried out as described previously (65). Rat α-tubulin antibody (Oxford Biotechnology) and fluorescein isothiocyanate-conjugated α-rat antibody (Jackson ImmunoResearch) were diluted at 1:200 and 1:100, respectively. Meiotic spreads were performed as described previously (42). α-Zip1 antibody (kindly provided by N. Kleckner) and fluorescein isothiocyanate-conjugated α-rabbit antibody (Jackson ImmunoResearch) were diluted at 1:150 and 1:50, respectively. Immunofluorescence samples were analyzed with a Zeiss Axioplan 2 microscope.

Immunoprecipitation and kinase assays. H1 kinase assays were performed as described previously (2). Briefly, Clb3-3HA protein was immunoprecipitated from 50 μl crude extract (250 μg total protein) using α-hemagglutinin (α-HA) antibody (Babco) and immunoglobulin G (IgG) Sepharose (Amersham Pharmacia). Sepharose beads were washed extensively with NP-40 buffer (50 mM Tris [pH 7.5], 150 mM NaCl, 1% NP-40) and 25 mM MOPS (morpholinepropanesulfonic acid [pH 7.0]). Beads were preincubated with 6 μl buffer HBII (25 mM MOPS, 15 mM $MgCl_2$, 5 mM EGTA, and 1 mM dithiothreitol, supplemented with protease and phosphatase inhibitors) for 15 min, before the addition of 10 μl kinase reaction mixture (25 mM MOPS, 2 mg/ml histone H1, 0.2 mM ATP) containing 50 nCi [γ-^{32}P]ATP. Kinase reactions were allowed to proceed for 15 min at 25°C before they were stopped by the addition of 10 μl 3× sodium dodecyl sulfate loading buffer. Samples were separated on a 15% sodium dodecyl sulfate-acrylamide gel, fixed in 10% methanol–10% acetic acid, dried, and analyzed by autoradiography.

Northern blot analysis. Northern blot analysis was performed as described previously (2). Total RNA was purified by phenol extraction and ethanol precipitation. A total of 10 μg RNA was loaded per lane and separated on a 1.1% agarose gel containing 6% formaldehyde and 40 mM MOPS (pH 7.0). Gels were blotted in 10× SSC (1× SSC is 0.15 M NaCl plus 0.015 M sodium citrate [pH = 7.0]) onto Hybond-XL membranes (Amersham Biosciences). Blots were probed overnight with randomly ^{32}P-labeled DNA probes typically spanning ~1 kb of the respective open reading frame.

cRNA target synthesis and microarray hybridization. Frozen yeast cell pellets stored at −80°C were quickly thawed and processed by the hot-phenol method (28). Approximately 190 μg of total RNA was isolated from 0.7×10^8 cells. Subsequently, 80 μg of total RNA was mixed with 350 μl RLT buffer and 250 μl of 70% ethanol. The mix was loaded onto an RNeasy Mini-Spin column

(QIAGEN), and RNA was eluted in 50 μl of double-distilled water. Total RNA quality was monitored by loading approximately 200 ng onto an RNA Nano 6000 Chip processed with the 2100 Bioanalyzer (Agilent) (see Fig. S1A, top, in the supplemental material). Biotin labeling of RNA was performed as described in the Expression Analysis Technical Manual (Affymetrix) with minor modifications as previously published (51). Approximately 80 μg of labeled cRNA from each reaction was purified using RNeasy Mini-Spin columns, and roughly 300 ng was analyzed on RNA Nano 6000 Chips (see Fig. S1A, bottom, in the supplemental material). A total of 220 μl of the hybridization mixture containing target cRNA at a final concentration of 0.05 μg/μl was transferred onto S98 GeneChips (Affymetrix) and incubated at 45°C on a rotator in a Hybridization Oven 640 (Affymetrix) for 16 h at 60 rpm. The arrays were washed, stained, and scanned as previously described (51). DAT (image), CEL (feature or oligonucleotide probe level), and TXT (gene or probe set level) files of the GeneChips were generated using an Agilent GeneArray scanner (low-intensity settings) and Microarray Analysis Suite 5.0 (Affymetrix).

Microarray data analysis. Raw data at the feature (oligonucleotide probe) level (CEL files) computed using the algorithm implemented in MAS 5.0 (Affymetrix) were imported into software packages available via the BioConductor project (http://www.bioconductor.org/). Data from CEL files were normalized, analyzed, and clustered using the R language for statistical computing (http://www.r-project.org) and the variance stabilization (VSN) algorithm (19) as implemented in the BioConductor package (http://bioconductor.org), following basic procedures as previously described (51). The Perfect Match values for all probes of a probe set were averaged to yield a single expression value for each gene represented on the array by employing the median polish algorithm as previously published (21). Oligonucleotide probes yielding questionable signals were marked during the image analysis, and the features (probes) at the 3′-most position of each probe set were disregarded during signal computation to decrease the effect of signal artifacts and RNA degradation on data quality (since cRNA synthesis proceeds in a 5′-to-3′ direction). A detailed documentation of all processing and analysis steps (30) is provided as supplemental material on our web portal at http://www.biozentrum.unibas.ch/primig/benomyl/, which provides access to web-specific figures, hyperlinked tables, supporting information, and raw data files. The file provides a code in the R programming language combined with comments in LATEX format. It can be downloaded together with the raw data as a single R package. Within R, the code can be extracted or a PDF document providing an overview of the analysis can be generated. A graphic display of the expression data for each locus is accessible via the GermOnline knowledgebase at http://www.germonline.org (43, 66, 67). A total of 1,189 transcripts that displayed a strong variation of signals between different samples compared to (theoretically) identical replicates were grouped using a hierarchical clustering algorithm (Euclidian distance) and sorted over signal strength during mitotic growth. To search for functional gene ontology (GO) annotations that are correlated with a particular expression pattern in a statistically significant manner, we employed the goCluster tool. Briefly, all loci for which reliable data are available (without prior filtration) are first grouped via their expression patterns using k-means clustering; subsequently, the genes bearing related functional annotation within each cluster are identified using a statistical test (G. Wrobel and M. Primig, submitted for publication). In addition, we directly identified a number of functionally related loci through other GO categories.

MIAME compliance. The TXT and CEL data files corresponding to cells in rich and presporulation medium (YPD and YPA), sporulation medium (SP4 and SF5), treated samples (SD5, SD8, SB5, and SB8), and cold-shocked samples as well as the appropriate controls (SR4, SR5, SR8, SC5, and SC8) were uploaded to the GEO (National Center for Biotechnology Information) public data repository at http://www.ncbi.nlm.nih.gov/geo/ (12). Files can be retrieved using the accession number GSE1693. CEL and TXT data files of all samples are also available at our web portal.

Other techniques. Spore viability was analyzed by dissection of tetrads. Flow cytometric analysis of total cellular DNA content and immunoblot analysis was performed as previously described (64). For immunoblotting, α-HA antibody (HA.11; Babco) was used at a 1:500 dilution, α-CLB3 (rabbit; Santa Cruz Biotechnology) was used at a 1:200 dilution, α-Cdc28 antibody was used at a 1:1,000 dilution, and α-Cdc2-Tyr15-P antibody (Cell Signaling Technology) was used at a 1:1,000 dilution. Pairing behavior of green fluorescent protein (GFP)-marked chromosomes was analyzed in vivo with a Zeiss Axioplan 2 microscope.

RESULTS

Benomyl reversibly arrests cells during meiosis. To study the consequences of microtubule perturbation on meiotic cell cycle progression and spore formation, we treated cells with the microtubule-depolymerizing drug benomyl. Previous reports indicated that a benomyl concentration of 60 μg/ml elicits a metaphase I delay in meiotic cells (56). We also observed a small delay in nuclear divisions at this concentration compared to a mock-treated culture (0.4% DMSO) (Fig. 1A). However, at 60 μg/ml, benomyl caused only incomplete microtubule depolymerization, and occasional short spindles were observed (data not shown). To more completely depolymerize microtubules, we incubated cells with 90 μg/ml or 120 μg/ml benomyl. The delay in nuclear division appeared more pronounced as the benomyl concentration was increased (Fig. 1B), with no cells undergoing nuclear divisions at the highest concentration of the spindle toxin, as was observed previously (58). In the presence of benomyl at 120 μg/ml, microtubules disappeared within minutes, and only the spindle pole bodies (SPBs) exhibited weak reactivity with anti-tubulin antibodies (Fig. 1C and D).

The benomyl concentration used in this analysis was three to eight times higher than the concentration typically used to arrest mitotically growing cells (35, 50). It was therefore important to determine that such high benomyl concentrations were not toxic to the cells. To investigate this, cells were incubated for 5 h with the compound, washed, and released into sporulation medium. Cells rapidly resumed the meiotic program, initiated meiotic spindle formation as judged by the separation of SPBs (Fig. 1E), and underwent the nuclear divisions with kinetics indistinguishable from mock-treated cells (Fig. 1F). Furthermore, the severe sporulation defect was reversed when benomyl was removed from the medium (Fig. 1G), and spore viability was indistinguishable from that of mock-treated cells (mock treated, 93%; benomyl-treated, 96%; 240 spores analyzed for each condition). Our results indicate that high levels of benomyl effectively inhibit progression through meiosis in a reversible manner without apparent adverse effects on meiotic cell cycle progression and spore formation.

Benomyl treatment prevents Clb-CDK accumulation in meiotic cells. Treatment of mitotically growing cells with 15 μg/ml benomyl causes cells to arrest in metaphase, with unseparated sister chromatids and high levels of mitotic (Clb) CDK activity (32). We obtained similar results when we increased this concentration to 120 μg/ml benomyl (Fig. 2A and B). To determine the effects of high levels of benomyl on meiotic cell cycle progression, we characterized the cell cycle arrest caused by addition of the drug. Exposure to 120 μg/ml benomyl caused cells to arrest with unseparated SPBs (Fig. 1D and 2C), as has been previously observed with mitotically growing cells treated with this drug (22). However, in contrast to mitotically growing cells, meiotic cells treated with benomyl during or after completion of S phase exhibited a dramatic delay in the accumulation of Clb3 protein and associated kinase activity (Fig. 2). Furthermore, Cdc28, the catalytic subunit of CDKs, was phosphorylated on tyrosine 19, which reflects a cell cycle arrest prior to entry into the chromosome segregation phase (41). Thus, whereas mitotic cells treated with high levels of benomyl arrest in metaphase, meiotic cells cultured under similar conditions during S phase and prophase arrested prior to the accumulation of Clb-CDKs that is necessary for entry into meiosis I.

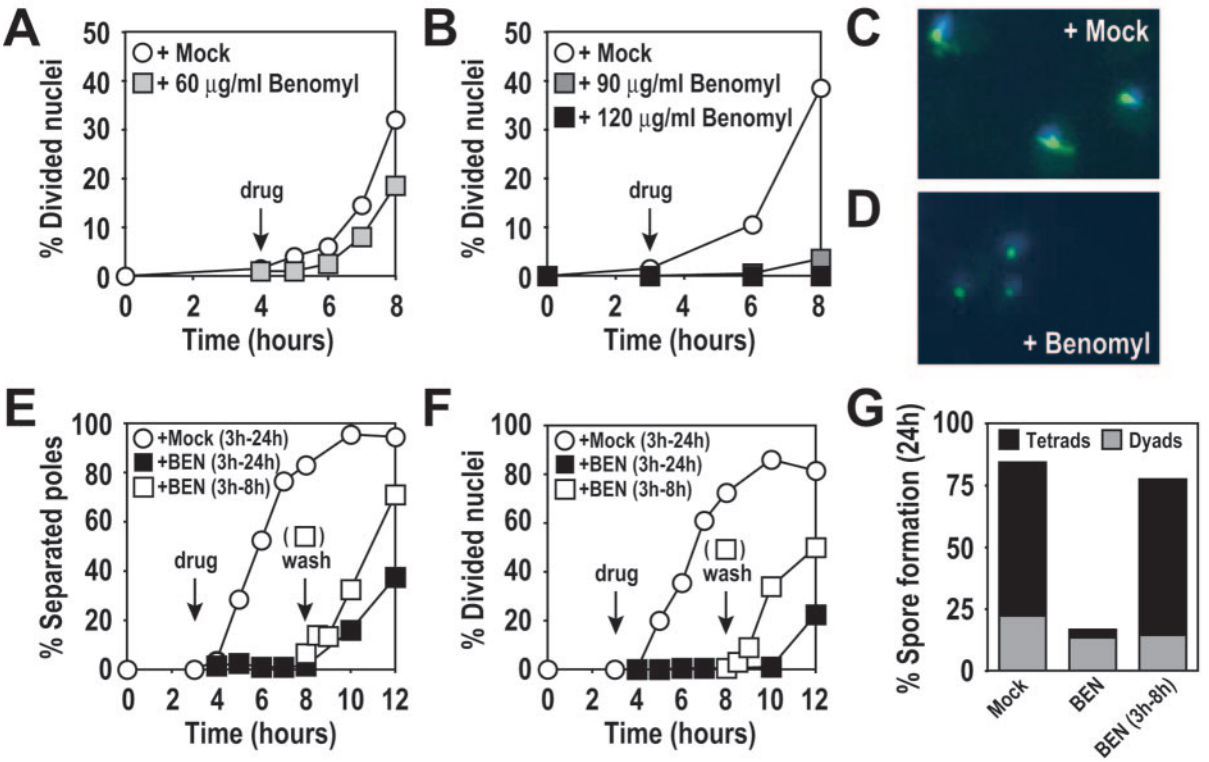

FIG. 1. High levels of benomyl reversibly arrest meiotic cells. (A) Wild-type (A727) cells. At 4 h after meiotic induction at room temperature (black arrow with the label "drug"), cells were resuspended in medium containing 60 μg/ml benomyl (grey squares) or 0.4% DMSO (mock; white circles). (B) Wild-type (A727) cells. At 3 h after meiotic induction at 30°C (black arrow), cells were resuspended in medium containing 90 μg/ml benomyl (dark grey squares), 120 μg/ml benomyl (black squares), or 0.4% DMSO (mock, white circles). The percentages of cells in the results shown in panels A and B that underwent at least one nuclear division were determined by DAPI (4′,6-diamidino-2-phenylindole) staining at the indicated time points. (C and D) Wild-type (A727) cells from cultures treated with 0.4% DMSO (C) or 120 μg/ml benomyl (D) fixed 1 h after treatment. DAPI-stained nuclear masses are shown in blue, and tubulin is shown in green. (E to G) Wild-type (A727) cells. At 3 h after meiotic induction at 30°C (arrow with the label "drug"), cells were resuspended in medium containing 120 μg/ml benomyl (black squares) or 0.4% DMSO (mock; white circles). At 5 h after drug addition (arrow labeled "wash"), the benomyl culture was split, and half the culture was washed and released into fresh sporulation medium containing 0.4% DMSO (white squares). (E) Percentage of cells containing more than one focus of tubulin staining. (F) Percentage of cells having undergone nuclear divisions (DAPI). (G) Spore formation 24 h after induction of meiosis. Asci were classified as containing two spores (dyads) or three or four spores (tetrads) (500 cells were analyzed for each condition).

Chromosome pairing is defective in the presence of high levels of benomyl. To further characterize the arrest induced by high levels of benomyl, we examined chromosome pairing and synapsis. Homologous chromosomes align during prophase, and this process is completed when a multilayered structure, the SC, has formed between homologs (48, 71). We spread meiotic nuclei at various time points before and after benomyl addition and stained them with an antibody against the SC component Zip1 (59). The appearance of the first Zip1 foci was noticeably delayed in benomyl-treated cells compared to mock-treated cells, and SC formation along the entire length of chromosomes was even further delayed (Fig. 3A).

To examine the effects of benomyl on homolog pairing, we integrated tandem arrays of the Tet operator sequence (*tetO*) at the *LEU2* locus on chromosome III (*LEU2* arrays) or at the *URA3* locus on chromosome V (*URA3* arrays). The arrays were visualized by expressing a Tet repressor (TetR)-GFP fusion protein, which binds to the *tetO* arrays (38). To assay pairing, we created diploid cells with *LEU2* arrays on both copies of chromosome III, which allowed us to analyze the behavior of a homologous locus. We assessed pairing by determining whether one or two GFP dots were visible within the cell. In this assay, only one GFP dot was visible if the arrays were paired or closely associated. As a control for nonspecific array clustering, we also examined diploid strains with one *LEU2* array and one *URA3* array, i.e., the two arrays were at nonhomologous positions. Around or shortly after premeiotic S phase (3-h time point), the homologous loci appeared more or less randomly arranged with respect to each other, since colocalization of *LEU2*/*LEU2* (homologous) occurred at similar frequency as colocalization of *LEU2*/*URA3* (nonhomologous) (Fig. 3B). In the mock-treated culture, the homologous *LEU2* loci increasingly colocalized during prophase, reaching maximal pairing 6 h after transfer into sporulation medium. Pairing was then lost as cells completed the first meiotic division. The nonhomologous *LEU2*/*URA3* combination, on the other hand, exhibited a slight drop in colocalization, presumably because the ongoing homolog alignment restricted random colocalization of nonhomologous sequences. In the benomyl-treated culture, association of homologous *LEU2* loci was very much delayed (Fig. 3B). Thus, this delay in homolog pairing correlated well with the effect of benomyl on SC formation (Fig.

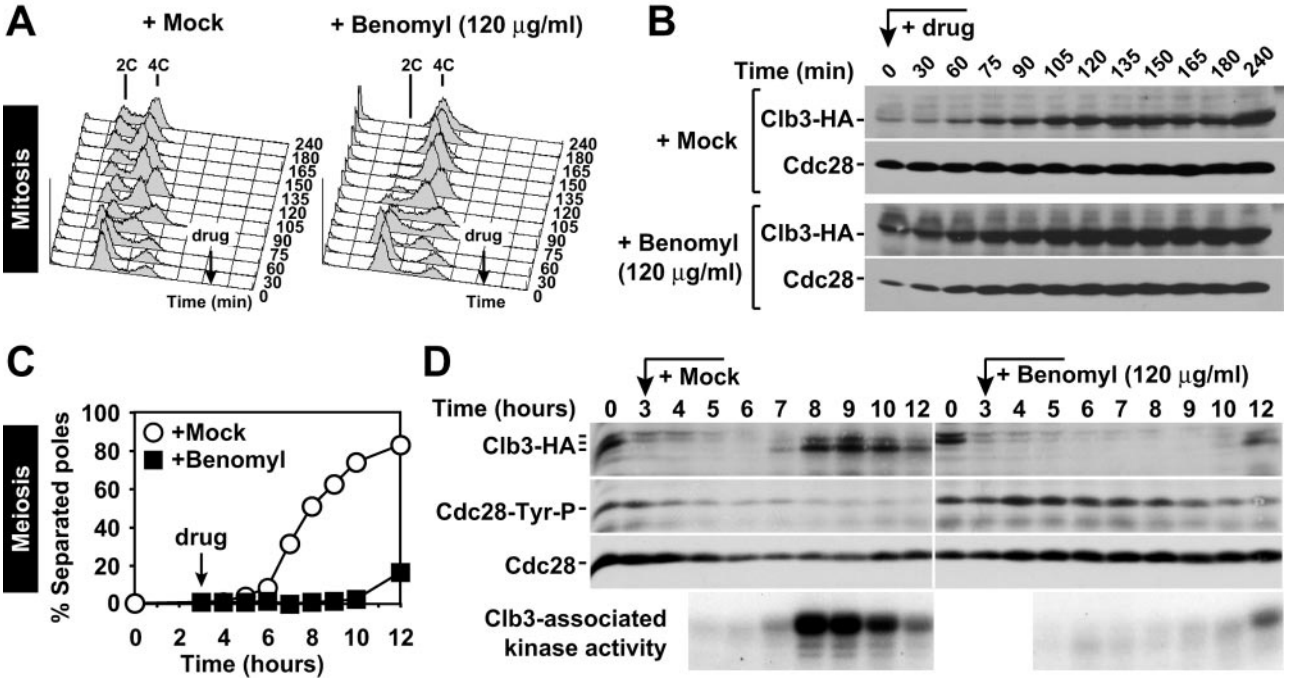

FIG. 2. Meiotic cells arrest with low levels of Clb3 protein and low Clb3-associated kinase activity. (A and B) Wild-type cells carrying a *CLB3-3HA* fusion (A4563) were enriched in G_1 by acetate starvation and released into YPD medium containing 0.4% DMSO (panel A, left) or 120 μg/ml benomyl (panel A, right). (A) Total cellular DNA content determined by flow cytometry. Black arrows indicate the time of drug addition. (B) Western blot analysis of Clb3 and Cdc28 (loading control). (C and D) Wild-type cells carrying a *CLB3-3HA* fusion (A4563) at room temperature. At 3 h after meiotic induction (black arrow), cells were resuspended in medium containing 120 μg/ml benomyl (black squares) or 0.4% DMSO (mock; white circles). (C) Percentage of cells containing more than one focus of tubulin staining. (D) Western blot analysis of Clb3 (top panel), Cdc28 tyrosine 19 phosphorylation (second panel), and Cdc28 (loading control, third panel from top), and autoradiogram of H1-kinase activity of Clb3-3HA immunoprecipitated from crude extracts (bottom).

3A). Our results indicate that benomyl interferes with the pairing and synapsis of homologous sequences during meiosis.

Benomyl treatment causes cells to arrest in G_1 or G_2. Our results suggest addition of benomyl during or shortly after S phase triggers a cell cycle arrest in G_2. We next analyzed in more detail, whether benomyl affected the progression through S phase. To examine the effects of benomyl on premeiotic S phase, we determined the DNA content of benomyl-treated cells. Cells were induced to sporulate, and after 4 h benomyl was added. Progression through premeiotic S phase was not affected by benomyl. The 4C peak continued to increase for at least 1 h after benomyl addition (Fig. 4A to C). Quantification of the extent of DNA replication occurring within an hour of mock or benomyl treatment showed that the extent of DNA replication was similar in the two cultures (Fig. 4A). We did, however, notice that an unusually high fraction of cells with a 2C DNA content persisted in the culture at later time points after benomyl addition (Fig. 4B and C). This finding raised the possibility that the initiation of DNA replication was inhibited by benomyl. Thus, due to the partial asynchrony of sporulating cultures, some cells had not yet started premeiotic S phase at the point of benomyl addition, and these lagging cells were prevented from entering premeiotic S phase by benomyl treatment. To test this possibility, we analyzed the consequences on meiotic progression when benomyl was added to a meiotic culture at the time of meiotic induction (time = 0 h). Analysis of this culture revealed that exposure to benomyl markedly delayed premeiotic DNA synthesis. This delay was due to a defect in entry into the meiotic program because accumulation of an early meiosis-specific protein, Rec8 (27), was significantly delayed (Fig. 4D).

The failure of benomyl-treated cells to enter into the meiotic cell cycle was not due to a general toxicity of the drug but was mediated by the absence of microtubules. Cells harboring the benomyl-dependent allele of β-tubulin *tub2-150* form overly stable microtubules that need to be destabilized by supplementation of the growth medium with at least 40 μg/ml benomyl (35, 62). Despite this need for benomyl, cells harboring the *tub2-150* allele were still sensitive to high doses of benomyl and grew very slowly in medium containing 120 μg/ml benomyl (data not shown). We reasoned, however, that this allele would allow us to shift the sensitivity curve compared to wild-type cells, making the response to benomyl less severe. As described below, cells carrying the *tub2-150* allele entered S phase in the presence of the drug (Fig. 5C). Thus, the arrest prior to premeiotic S phase was dependent on microtubule depolymerization. Our results indicate that benomyl causes two cell cycle arrests. It prevents entry into the first meiotic division if the drug is administered during or after premeiotic S phase and entry into the meiotic cell cycle if benomyl is administered during G_1.

High levels of benomyl interfere with gene expression during meiosis. The observation that benomyl, added before meiotic induction, caused a significant delay in the production of

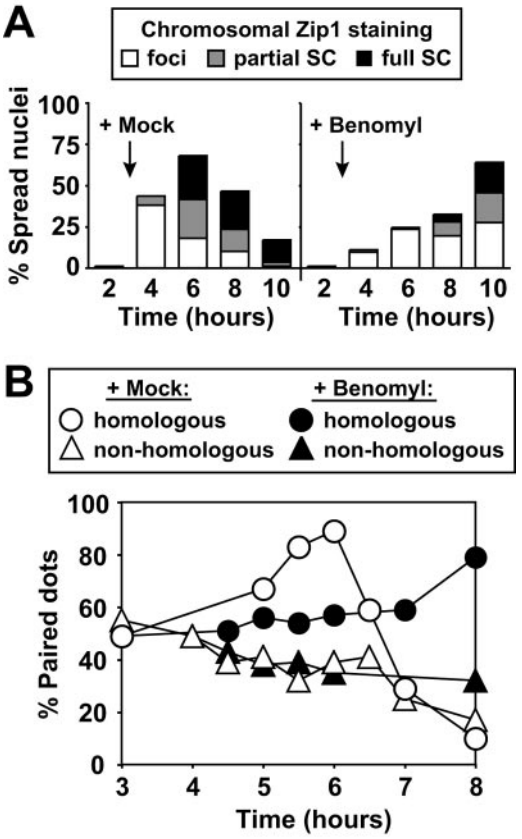

FIG. 3. Benomyl exposure causes delayed homolog pairing and SC formation. (A) Cells from the experiment shown in Fig. 2C and D were surface spread and stained for Zip1. The spread nuclei were classified based on the presence of no staining, dispersed Zip1 foci (white), elongated Zip1 foci (partial SC; grey), or Zip1 fully covering chromosomes (full SC; black). Black arrows indicate the time of drug addition. A total of 200 nuclei were counted for each time point. (B) Wild-type cells carrying *tetO* arrays at homologous (A5009; circles) or nonhomologous (A4967; triangles) chromosomal positions. At 3 h after meiotic induction at room temperature, cells were resuspended in medium containing 120 μg/ml benomyl (black symbols) or 0.4% DMSO (mock; white symbols). Pairing was determined with 100 live cells at the indicated time points. Chromosomes were considered unpaired if two clearly separated GFP dots were visible and paired if the two GFP dots were partially or fully overlapping.

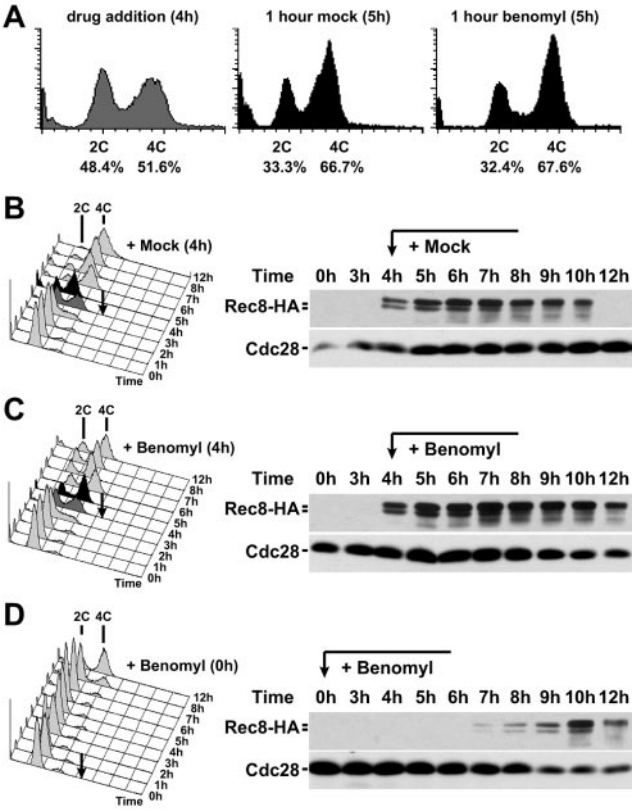

FIG. 4. Benomyl treatment does not affect premeiotic S phase but prevents entry into meiosis. Wild-type cells carrying a *REC8-3HA* fusion (A1972) are shown. At 4 h after meiotic induction at room temperature (black arrow), cells were resuspended in medium containing 0.4% DMSO (mock) (B) or 120 μg/ml benomyl (C). Total cellular DNA content was determined by flow cytometry (left). Dark grey cytometry profiles indicate time of drug addition (4 h); black profiles are from 1 h after drug addition (5 h). Western blot samples were used to monitor Rec8 levels during the same time course. (A) Percentages of cells with 2C and 4C DNA content at 4 h and 5 h were determined by quantifying the area beneath the respective peaks ± one-half the respective interpeak distance. (D) Cells were treated as in the experiment described in panel C, except that cells were resuspended directly into sporulation medium containing 120 μg/ml benomyl at the start of the meiotic time course.

the meiosis-specific protein, Rec8, raised the possibility that the drug interfered with transcription and/or translation of meiotic factors. To address this possibility, we analyzed RNA levels of the meiosis specific gene *IME2* (15). Consistent with the delayed accumulation of Rec8 protein, we also observed delayed accumulation of *IME2* mRNA, when benomyl was added at the time of meiotic induction (Fig. 5A). This result suggests that benomyl causes an arrest in G_1 by interfering with the accumulation of these two and perhaps other early meiotic cell cycle regulators.

To determine whether the benomyl-induced G_2 arrest was accompanied by transcriptional down-regulation, we analyzed the consequences of adding benomyl 4 h after transfer into meiosis-inducing conditions. mRNA levels of *IME2* and the cell cycle regulator *CLB5* dropped sharply upon benomyl addition (Fig. 5B). Surprisingly, mRNA levels of two constitutively expressed genes, *CDC28* and *RPL3*, showed a similar response, while expression of the large rRNA and the small nuclear RNA *SNR6* remained unchanged upon benomyl addition (Fig. 5B). Our results suggest that benomyl treatment during G_1 or S phase/G_2 leads to changes in meiotic gene expression, with a number of important cell cycle genes being drastically down-regulated.

The down-regulation of meiotic transcripts depends at least in part on microtubule depolymerization. To determine whether the decline in mRNA levels brought about by benomyl was due to the microtubule-depolymerizing effect of the drug, we examined the consequences of benomyl treatment on *IME2* mRNA levels in *tub2-150* cells (35, 62). Cells carrying the *tub2-150* allele were grown in the presence of 50 μg/ml benomyl and upon transfer into meiosis-inducing medium were incubated with 120 μg/ml benomyl. *tub2-150* cells entered the meiotic cell cycle normally, and *IME2* mRNA accumulated to

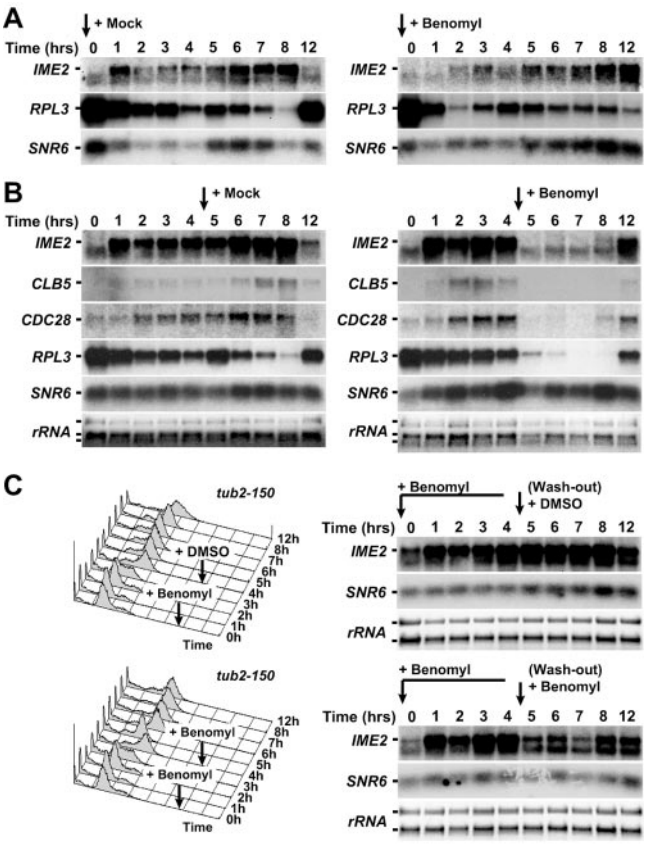

FIG. 5. Benomyl treatment triggers changes in meiotic gene expression. (A) Northern blot analysis of *IME2*, *RPL3*, and *SNR6* RNA levels. Wild-type cells (A1972) induced to undergo meiosis at room temperature in medium containing 0.4% DMSO (mock) (left) or 120 μg/ml benomyl (right). (B) The same strain as is shown in panel A was allowed to progress through meiosis for 4 h. After 4 h (black arrow), cells were resuspended in medium containing 0.4% DMSO (mock,) (left) or 120 μg/ml benomyl (right). Northern blot analysis of *IME2*, *CLB5*, *CDC28*, *RPL3*, and *SNR6* RNA levels was carried out; rRNA was used as a loading control. rRNA levels were determined by staining with ethidium bromide; all other RNAs were detected by autoradiography. (C) *tub2-150* cells (A5779) were pregrown at 30°C in medium containing 50 μg/ml benomyl and then sporulated at room temperature in medium containing 120 μg/ml benomyl. After 4 h, cells were resuspended in fresh medium containing 0.4% DMSO (mock) (top) or 120 μg/ml benomyl (bottom). Total RNA samples were analyzed by Northern blotting. Mock and benomyl-treated samples were run in the same gel but are separated in these figures for clarity. Total DNA content was analyzed by flow cytometry.

normal levels (Fig. 5C). When benomyl was removed after 4 h and cells were transferred into medium lacking the drug, *IME2* mRNA levels did not increase further, indicating that transcription was fully induced in the presence of high levels of benomyl (Fig. 5C). When benomyl was added again at a concentration of 120 μg/ml (during or after completion of DNA replication; time = 4 h), *IME2* expression decreased somewhat, although not nearly as dramatically as in wild-type cells (compare Fig. 5B and C). These results suggest that the decline in *IME2* RNA levels (and presumably that of other transcripts) brought about by benomyl is at least in part due to the microtubule-depolymerizing effect of the drug.

Benomyl causes a global change in meiotic gene expression. A large number of genes, including loci that are also involved in mitotic growth, are differentially regulated as cells progress through meiosis (52). Previous work has identified at least seven broad meiotic expression profiles, six of which involve transient up-regulation of transcription during the process (7, 44). To determine how general the effects of benomyl on gene expression were, we examined the effect of benomyl on meiotic gene expression at a genome-wide level as cells progressed through meiosis in the presence or absence of benomyl. The experimental protocol is outlined in Fig. 6A. Duplicate samples were harvested from cultures at several stages in premeiotic and meiotic development: after saturation in rich medium (YPD), after acetate starvation (YPA), and 4 h after induction of meiosis (SP4). At this point, cells were filtered and resuspended in normal SPO medium or in medium containing DMSO or benomyl. Duplicate samples were then harvested 1 h later from the SPO culture (SF5), DMSO culture (SD5), or benomyl culture (SB5) and 4 h later from the DMSO culture (SD8) or benomyl culture (SB8).

Total RNA samples from these time points were hybridized to Affimetrix S98 GeneChips covering approximately 6,400 yeast transcripts. A total of 1,189 transcripts displayed a strong variation of signals between different samples. These loci were grouped using a hierarchical clustering algorithm and sorted by signal strength during mitotic growth, such that genes strongly expressed in rich medium and presporulation medium were preferentially placed on top of the cluster (see Fig. S2 in the supplemental material). To get an overview of the gene functions dominating the different subparts of the hierarchical clustering, we used the goCluster tool to identify nonoverlapping branches of the hierarchical tree that showed the strongest enrichment of genes annotated with a common GO term (15a). The effects of benomyl were most obvious 1 h after drug addition, comparing DMSO-treated (SD5) with benomyl-treated (SB5) cells (Fig. 6; see also Fig. S2 in the supplemental material). A substantial number of genes were up-regulated by benomyl treatment in a highly coordinated manner, notably, genes encoding factors involved in drug response and transport (GO:0015893, drug transport; GO:0050896, response to stimulus), as well as subunits of the proteasome and genes required for ubiquitin-dependent proteolysis (GO:0006511, ubiquitin-dependent protein catabolism). Among the genes whose expression decreased in the presence of benomyl, we identified a large number of genes involved in protein translation (GO:0006412, protein biosynthesis), and factors implicated in meiotic development (GO:0030437, sporulation [sensu fungi]; GO:0030476, spore wall assembly [sensu fungi]; and GO:030154, cell differentiation). This suggests that benomyl treatment up-regulates genes involved in protein turnover and the response to stress, while negatively affecting many factors involved in cell growth and the cell cycle. Analysis of the transcriptional effects of benomyl on mitosis also showed an up-regulation of stress response genes and transporters; but in contrast to the meiotic cell cycle, no transcripts were down-regulated (S. Biggins, personal communication).

We then analyzed the transcriptional effects of benomyl on individual genes within those functional groups. In addition to causing an up-regulation of genes involved in protein turnover, the presence of benomyl led to a detoxification response. In

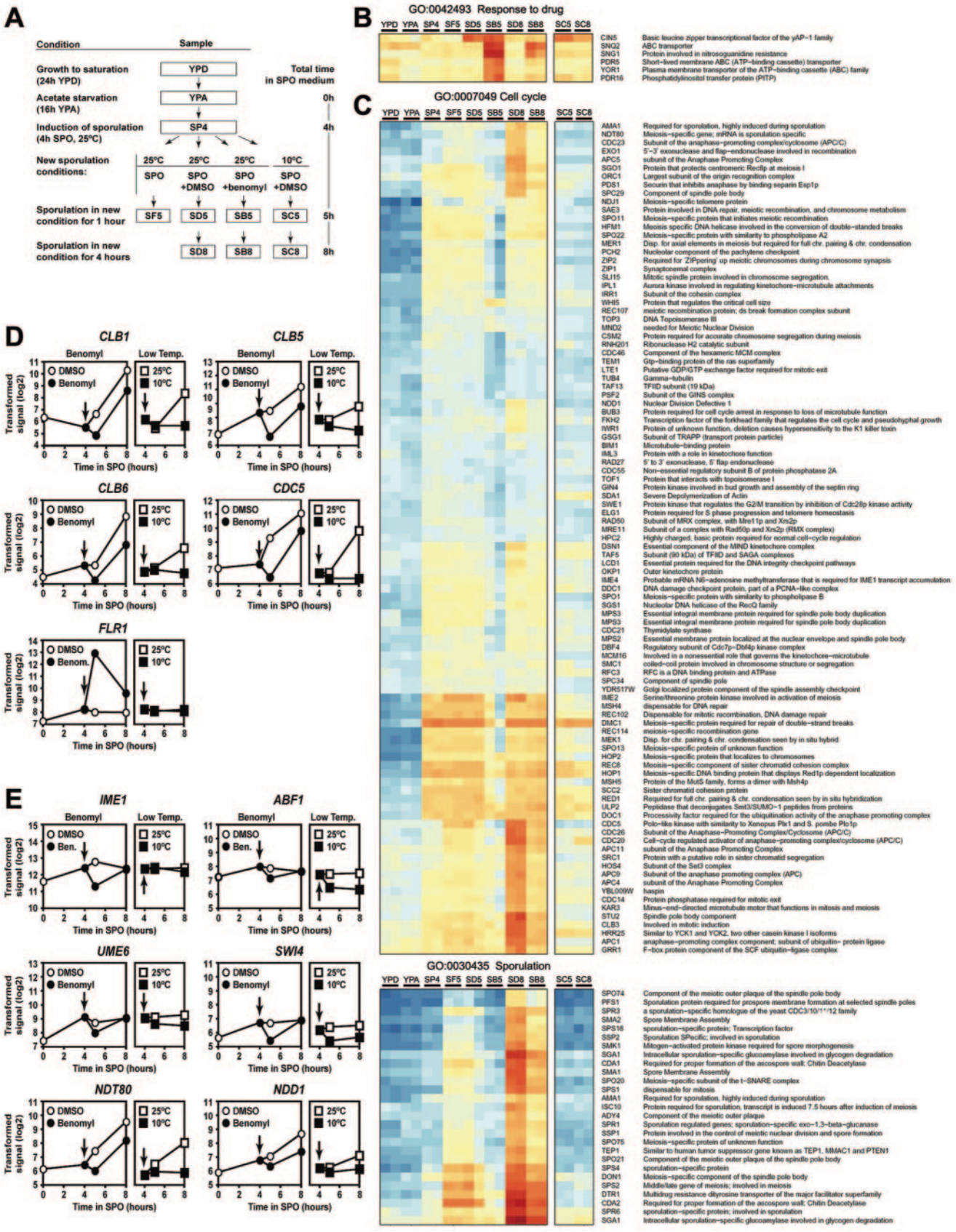
A
Condition
Sample
Growth to saturation (24h YPD)
YPD
Total time in SPO medium
Acetate starvation (16h YPA)
YPA
0h
Induction of sporulation (4h SPO, 25°C)
SP4
4h
New sporulation conditions:
25°C SPO
25°C SPO +DMSO
25°C SPO +benomyl
10°C SPO +DMSO
Sporulation in new condition for 1 hour
SF5
SD5
SB5
SC5
5h
Sporulation in new condition for 4 hours
SD8
SB8
SC8
8h
B
GO:0042493 Response to drug
YPD YPA SP4 SF5 SD5 SB5 SD8 SB8 SC5 SC8
CIN5 Basic leucine zipper transcriptional factor of the yAP-1 family
SNQ2 ABC transporter
SNG1 Protein involved in nitrosoguanidine resistance
PDR5 Short-lived membrane ABC (ATP-binding cassette) transporter
YOR1 Plasma membrane transporter of the ATP-binding cassette (ABC) family
PDR16 Phosphatidylinositol transfer protein (PITP)
C
GO:0007049 Cell cycle
YPD YPA SP4 SF5 SD5 SB5 SD8 SB8 SC5 SC8
AMA1 Required for sporulation, highly induced during sporulation
NDT80 Meiosis-specific gene; mRNA is sporulation specific
CDC20 Subunit of the anaphase-promoting complex/cyclosome (APC/C)
EXO1 5'-3' exonuclease and flap-endonuclease involved in recombination
APC5 subunit of the Anaphase Promoting Complex
SGO1 Protein that protects centromeric Rec8p at meiosis I
ORC1 Largest subunit of the origin recognition complex
PDS1 Securin that inhibits anaphase by binding separin Esp1p
SPC29 Component of spindle pole body
NDJ1 Meiosis-specific telomere protein
SAE3 Protein involved in DNA repair, meiotic recombination, and chromosome metabolism
SPO11 Meiosis-specific protein that initiates meiotic recombination
HFM1 Meiosis specific DNA helicase involved in the conversion of double-stanided breaks
SPO22 Meiosis-specific protein with similarity to phospholipase A2
MER1 Disp. for axial elements in meiosis but required for full chr. pairing & chr. condensation
PCH2 Nucleolar component of the pachytene checkpoint
ZIP2 Required for 'ZIPpering' up meiotic chromosomes during chromosome synapsis
ZIP1 Synaptonemal complex
SLI15 Mitotic spindle protein involved in chromosome segregation.
IPL1 Aurora kinase involved in regulating kinetochore-microtubule attachments
IRR1 Subunit of the cohesin complex
WHI5 Protein that regulates the critical cell size
REC107 meiotic recombination protein; ds break formation complex subunit
TOP3 DNA Topoisomerase III
MND2 needed for Meiotic Nuclear Division
CSM2 Protein required for accurate chromosome segregation during meiosis
RNH201 Ribonuclease H2 catalytic subunit
CDC46 Component of the hexameric MCM complex
TEM1 Gtp-binding protein of the ras superfamily
LTE1 Putative GDP/GTP exchange factor required for mitotic exit
TUB4 Gamma-tubulin
TAF13 TFIID subunit (19 kDa)
PSF2 Subunit of the GINS complex
NDD1 Nuclear Division Defective 1
BUB3 Protein required for cell cycle arrest in response to loss of microtubule function
FKH2 Transcription factor of the forkhead family that regulates the cell cycle and pseudohyphal growth
IWR1 Protein of unknown function, deletion causes hypersensitivity to the K1 killer toxin
GSG1 Subunit of TRAPP (transport protein particle)
BIM1 Microtubule-binding protein
IML3 Protein with a role in kinetochore function
RAD27 5' to 3' exonuclease, 5' flap endonuclease
CDC55 Non-essential regulatory subunit B of protein phosphatase 2A
TOF1 Protein that interacts with topoisomerase I
GIN4 Protein kinase involved in bud growth and assembly of the septin ring
SDA1 Severe Depolymerization of Actin
SWE1 Protein kinase that regulates the G2/M transition by inhibition of Cdc28p kinase activity
ELG1 Protein required for S phase progression and telomere homeostasis
RAD50 Subunit of MRX complex, with Mre11p and Xrs2p
MRE11 Subunit of a complex with Rad50p and Xrs2p (MRX complex)
HPC2 Highly charged, basic protein required for normal cell-cycle regulation
DSN1 Essential component of the MIND kinetochore complex
TAF5 Subunit (90 kDa) of TFIID and SAGA complexes
LCD1 Essential protein required for the DNA integrity checkpoint pathways
OKP1 Outer kinetochore protein
IME4 Probable mRNA N6-adenosine methyltransferase that is required for IME1 transcript accumulation
DDC1 DNA damage checkpoint protein, part of a PCNA-like complex
SPO1 Meiosis-specific protein with similarity to phospholipase B
SGS1 Nucleolar DNA helicase of the RecQ family
MPS3 Essential integral membrane protein required for spindle pole body duplication
MPS3 Essential integral membrane protein required for spindle pole body duplication
CDC21 Thymidylate synthase
MPS2 Essential membrane protein localized at the nuclear envelope and spindle pole body
DBF4 Regulatory subunit of Cdc7p-Dbf4p kinase complex
MCM16 Involved in a nonessential role that governs the kinetochore-microtubule
SMC1 coiled-coil protein involved in chromosome structure or segregation
RFC3 RFC is a DNA binding protein and ATPase
SPC34 Component of spindle pole
YDR517W Golgi localized protein component of the spindle assembly checkpoint
IME2 Serine/threonine protein kinase involved in activation of meiosis
MSH4 dispensable for DNA repair
REC102 Dispensable for mitotic recombination, DNA damage repair
DMC1 Meiosis-specific protein required for repair of double-strand breaks
REC114 meiosis-specific recombination gene
MEK1 Disp. for chr. pairing & chr. condensation seen by in situ hybrid
SPO13 Meiosis-specific protein of unknown function
HOP2 Meiosis-specific protein that localizes to chromosomes
REC8 Meoisis-specific component of sister chromatid cohesion complex
HOP1 Meiosis-specific DNA binding protein that displies Red1p dependent localization
MSH5 Protein of the MutS family, forms a dimer with Msh4p
SCC2 Sister chromatid cohesion protein
RED1 Required for full chr. pairing & chr. condensation seen by in situ hybridization
ULP2 Peptidase that deconjugates Smt3/SUMO-1 peptides from proteins
DOC1 Processivity factor required for the ubiquitination activity of the anaphase promoting complex
CDC5 Polo-like kinase with similarity to Xenopus Plx1 and S. pombe Plo1p
CDC26 Subunit of the Anaphase-Promoting Complex/Cyclosome (APC/C)
CDC20 Cell-cycle regulated activator of anaphase-promoting complex/cyclosome (APC/C)
APC11 subunit of the Anaphase Promoting Complex
SRC1 Protein with a putative role in sister chromatid segregation
HOS4 Subunit of the Set3 complex
APC9 Subunit of the anaphase promoting complex (APC)
APC4 subunit of the Anaphase Promoting Complex
YBL009W haspin
CDC14 Protein phosphatase required for mitotic exit
KAR3 Minus-end-directed microtubule motor that functions in mitosis and meiosis
STU2 Spindle pole body component
CLB3 Involved in mitotic induction
HRR25 Similar to YCK1 and YCK2, two other casein kinase I isoforms
APC1 anaphase-promoting complex component; subunit of ubiquitin- protein ligase
GRR1 F-box protein component of the SCF ubiquitin-ligase complex
GO:0030435 Sporulation
YPD YPA SP4 SF5 SD5 SB5 SD8 SB8 SC5 SC8
SPO74 Component of the meiotic outer plaque of the spindle pole body
PFS1 Sporulation protein required for prospore membrane formation at selected spindle poles
SPR3 a sporulation-specific homologue of the yeast CDC3/10/11/12 family
SMA2 Spore Membrane Assembly
SPS18 sporulation-specific protein; Transcription factor
SSP2 Sporulation SPecific; involved in sporulation
SMK1 Mitogen-activated protein kinase required for spore morphogenesis
SGA1 Intracellular sporulation-specific glucoamylase involved in glycogen degradation
CDA1 Required for proper formation of the ascospore wall; Chitin Deacetylase
SMA1 Spore Membrane Assembly
SPO20 Meiosis-specific subunit of the t-SNARE complex
SPS1 dispensable for mitosis
AMA1 Required for sporulation, highly induced during sporulation
ISC10 Protein required for sporulation, transcript is induced 7.5 hours after induction of meiosis
ADY4 Component of the meiotic outer plaque
SPR1 Sporulation regulated genes; sporulation-specific exo-1,3-beta-glucanase
SSP1 Protein involved in the control of meiotic nuclear division and spore formation
SPO75 Meiosis-specific protein of unknown function
TEP1 Similar to human tumor suppressor gene known as TEP1, MMAC1 and PTEN1
SPO21 Component of the meiotic outer plaque of the spindle pole body
SPS4 sporulation-specific protein
DON1 Meiosis-specific component of the spindle pole body
SPS2 Middle/late gene of meiosis; involved in meiosis
DTR1 Multidrug resistance dityrosine transporter of the major facilitator superfamily
CDA2 Required for proper formation of the ascospore wall; Chitin Deacetylase
SPR6 sporulation-specific protein; involved in sporulation
SGA1 Intracellular sporulation-specific glucoamylase involved in glycogen degradation
D
CLB1
CLB5
CLB6
CDC5
FLR1
Benomyl
Low Temp.
DMSO
Benomyl
Benom.
25°C
10°C
Transformed signal (log2)
Time in SPO (hours)
E
IME1
ABF1
UME6
SWI4
NDT80
NDD1
Ben.

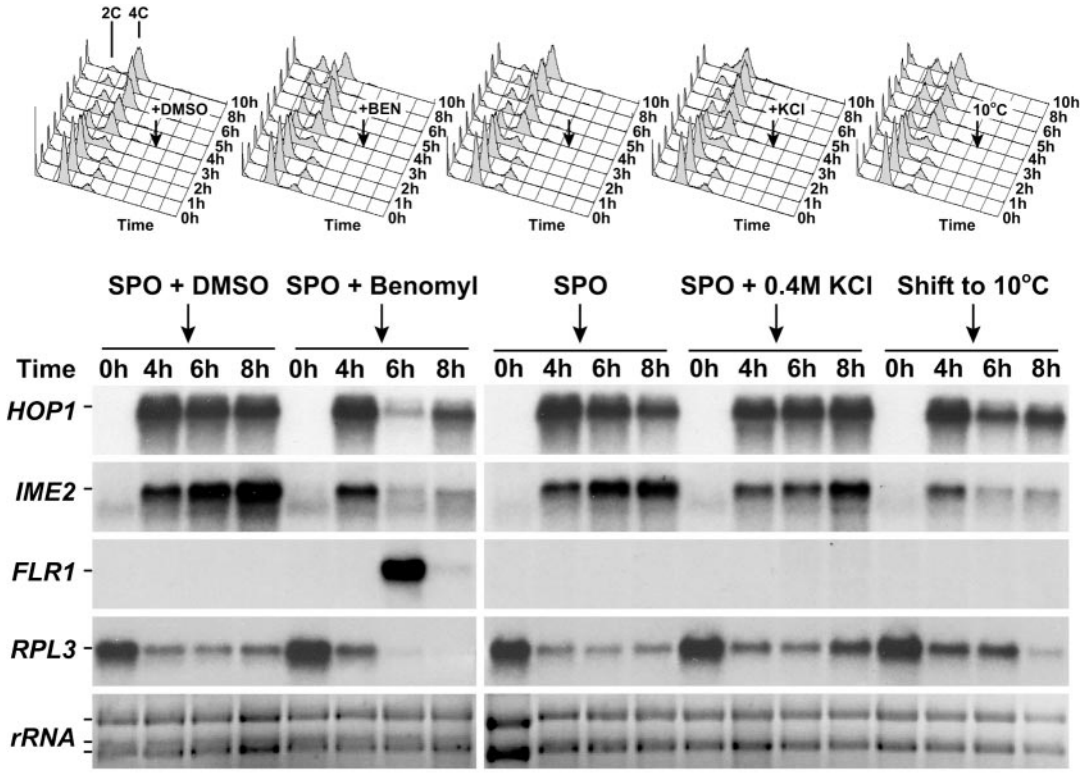

FIG. 7. Benomyl-induced changes in meiotic gene expression are not a general stress response but resemble the transcriptional response to low temperatures. At 4 h after induction of meiosis at room temperature (black arrows), wild-type cells (A1972) were either cultured at room temperature in SPO medium containing various additives (0.4% DMSO, 0.4% DMSO plus 120 μg/ml benomyl, no additive, or 0.4 M potassium chloride) or cultured at 10°C. Cellular DNA content was determined by flow cytometry (top panels). Total RNA samples were analyzed by Northern blotting (bottom panels). All samples were run in the same gel but are separated in this figure for clarity.

particular, we observed increased expression of genes involved in transport (*SNQ2* and *YOR1*), multidrug and chemical stress resistance (*CIN5*, *PDR5*, *PDR16*, and *SNG1*) (Fig. 6B), and stress response, including *FLR1*, a gene encoding a benomyl-inducible multidrug resistance permease (Fig. 7). At the same time, benomyl treatment caused a widespread down-regulation of meiosis-specific genes and general cell cycle factors (Fig. 6C). These include genes essential for meiotic transcriptional control (*IME2*, *IME4*, and *NDT80*) and early meiotic functions, such as recombination (*EXO1*, *MSH4*, *MSH5*, *REC102*, *REC107*, *REC114*, *SAE3*, and *SPO11*), SC formation (*HOP1*, *HOP2*, *MND1*, *MER1*, *RED1*, *ZIP1*, and *ZIP2*), sister chromatid cohesion and chromosome segregation (*CSM2*, *IRR1*/*SCC3*, *REC8*, *SCC2*, and *SGO1*), spindle pole body formation (*SPO1*), the recombination checkpoint (*PCH2*, *MEK1*, and *DDC1*), and control of M phase (*CDC5*, *MND2*, and *SPO13*). As a consequence of the decreased expression of early meiotic genes, factors involved in postmeiotic functions like spore wall formation and maturation (e.g., *ADY4*, *DON1*, *SMA1*, *SMK1*, *SPO74*, *SPR3*, *SPR6*, and *SSP2*) were also expressed later and

FIG. 6. Benomyl treatment triggers a transcriptional response from genes involved in detoxification, cell cycle control, and the meiotic program. (A) Flow chart of the experimental protocol. Boxes indicate the samples analyzed in the results shown in Fig. 6 (see also Fig. S2 in the supplemental material). Box labels correspond to column labels in panels B and C. The flow chart also indicates the total time cultures spent in sporulation (SPO) medium. The time spent in SPO medium corresponds to the *x* axis of the graphs shown in panels D and E. (B and C) Loci involved in drug response and mitotic or meiotic cell cycles, as well as sporulation. The complete data set was analyzed using goCluster and split into 100 subgroups with similar expression using partitioning around medoids (26). The GO categories associated with the genes in each of the resulting groups were analyzed for statistically significant overrepresentation by comparing the frequencies of occurrence of the same GO term within the group and all transcripts represented on the microarray, respectively. The hypergeometric distribution was employed to determine the resulting *P* values (18). To correct for the multiple testing procedure, we used data from 100 randomized data sets to determine a *P* value cutoff that would result in a false discovery rate of 10%. A total of 586 different GO terms were identified as being enriched in one or several of the 100 clusters. Blue and red indicate low and high expression values, respectively. (D and E) Expression patterns of manually selected genes involved in drug response, cell cycle control and the regulation of mitotic and meiotic gene expression. Signals are given as $\log_2$ transformed values on the *y* axis and are graphed versus the total time the cultures spent in SPO medium. Black arrows indicate the time of drug treatment or shift to low temperature. Note that low abundance mRNAs that are also cell cycle regulated (e.g., *SWI4*) are often not or only barely detectable in nonsynchronized heterogeneously growing cell populations.

at a lower level. Among factors important for both mitotic and meiotic cell cycle progression, we observed coordinated transcriptional down-regulation of the protein kinase *CDC28*, five of its six B-type cyclin regulatory subunits (*CLB1*, *CLB3*, *CLB4*, *CLB5*, and *CLB6*; note that *CLB2* is not expressed during the meiotic cell cycle) (Fig. 6C and D), and components of the APC/C (*APC4*, *APC5*, *APC11*, *CDC20*, *CDC23*, and *CDC26*).

Microtubule depolymerization may affect the expression of this large group of genes by influencing the expression of a smaller set of transcription factors that regulate the former. To test this, we directly examined a number of transcription factors involved in stress response, cell cycle regulation, and meiotic expression. Indeed, we found that mRNA levels of several transcription factors, *SWI4*, *NDD1* (G_1- and G_2/M-specific induction), *ABF1* (general regulator of mitotic and meiotic genes), as well as *IME1*, *UME6*, and *NDT80* (required for meiotic activation and rerepression) were down-regulated at the transcriptional level in the presence of benomyl (Fig. 6E). This was not a general effect, since other transcription factors involved in stress response (Gcn4) and cell cycle control (Swi6, Mpb1, Mcm1, and Fkh1) did not show a significant decrease in their expression levels (see the *S. cerevisiae* section of Germ Online at http://www.germonline.org). These results suggest that the widespread transcriptional changes that occur after benomyl-induced microtubule destabilization could be correlated with the down-regulation of a set of transcription factors that regulate these genes.

Cold shock causes effects similar to those of benomyl. Low temperatures are also known to destabilize microtubules (14). To determine whether cold temperatures affected transcription in a manner similar to that of benomyl, we analyzed the transcriptional changes in sporulating cultures which, instead of being exposed to benomyl, were shifted to low temperatures (10°C) for 1 h (SC5) or 4 h (SC8). Low-temperature stress did not lead to induction of genes involved in detoxification and drug transport but did cause, among other effects, a general shutdown of the meiotic transcriptional program very similar to that observed with benomyl-treated cells (Fig. 6B and C). One notable exception is the transcription factor *IME1*, whose expression, while down-regulated by benomyl, does not appear to be markedly affected by low-temperature stress (Fig. 6E). Taken together, these results suggest that a wide array of genes involved in cell proliferation and meiotic progression, including the three major early meiotic kinases *IME2*, *CDC28*, and *CDC5* are down-regulated to halt cell cycle progression in the presence of damaged microtubules.

The down-regulation of meiotic genes by low temperatures or benomyl treatment was not caused by a general meiotic stress response pathway, because cells lacking the major stress kinase *HOG1* still arrested in G_2 after benomyl treatment (data not shown), and exposure of meiotic cells to hypertonic stress (0.4 M potassium chloride) did not elicit a change in gene expression comparable to that induced by benomyl or cold treatment. mRNA levels of *IME2*, *HOP1*, and *RPL3* declined after treatment with benomyl or exposure to cold but remained at normal levels after exposure to hypertonic stress (Fig. 7). Furthermore, cell cycle arrest occurred in either G_1 or G_2 after exposure to benomyl or low temperatures but not if cells were exposed to hypertonic stress (Fig. 7, top). On the other hand, expression analysis suggested that the detoxification response was benomyl specific. We confirmed this by analyzing expression of the multidrug resistance permease gene, *FLR1*, by Northern blot analysis (Fig. 7). Thus, microtubule perturbation (chemically or by low temperature) but not other stress causes a specific transcriptional response that leads to meiotic cell cycle arrest in G_1 or G_2.

G_2 arrest caused by benomyl treatment is independent of known meiotic checkpoints. Several checkpoints have been characterized to date that cause a cell cycle arrest prior to meiotic chromosome segregation. We therefore determined whether any of the known meiotic checkpoints were responsible for the G_2 arrest brought about by benomyl treatment. Since microtubule destabilization appeared to be the cause for the arrest, we first tested whether the G_2 arrest we observed was dependent on the spindle assembly checkpoint. Deletion of the spindle assembly checkpoint component *MAD2* did not bypass the G_2 arrest. *mad2*Δ cells treated with benomyl exhibited the same delay in Clb3 accumulation as wild-type cells (Fig. 8A). Thus, the G_2 arrest caused by benomyl treatment is not due to activation of the spindle checkpoint.

The recombination checkpoint (pachytene checkpoint) arrests cells in G_2 by down-regulating Clb-CDK activity and by inhibiting the transcription factor Ndt80 responsible for the transcriptional activation of genes necessary for entry into meiosis I and spore formation (49). Clb-CDK activity is kept low by at least two mechanisms. The protein kinase Swe1 phosphorylates Cdc28 on tyrosine 19, thereby inhibiting its activity (31). At the same time, *CLB* cyclin transcription is repressed through the inhibition of Ndt80 (63). To determine whether the recombination checkpoint is required for the G_2 arrest caused by benomyl treatment, we analyzed the response of *mek1*Δ and *swe1*Δ mutants to benomyl. Mek1 is the meiotic homolog of the mitotic DNA-damage checkpoint kinase Rad53 and a central player in the recombination checkpoint (3, 69). Cells lacking *MEK1* arrested with low levels of Clb3 protein after exposure to benomyl (Fig. 8B). Similar results were obtained when Swe1 was inactivated (Fig. 8A). We furthermore excluded the possibility that the recombination checkpoint and the spindle assembly checkpoint acted together to cause the arrest by examining the response of *mek1*Δ *mad2*Δ double mutants to benomyl treatment (Fig. 8C). Our results indicate that inactivation of both the recombination checkpoint and the spindle checkpoint does not allow benomyl-treated cells to enter meiosis I.

Finally, we tested whether the presence of unprocessed meiotic double-strand breaks contributed to the G_2 arrest caused by benomyl treatment. Cells lacking *RAD50* do not form meiotic double-strand breaks (6), yet they still arrested in G_2 with low levels of Clb3 protein upon exposure to benomyl (Fig. 8B). We conclude that the benomyl-triggered G_2 arrest is independent of double-strand break formation and is not due to activation of either the recombination or the spindle checkpoint.

DISCUSSION

Our analyses reveal a profound effect of microtubule destabilization on meiotic progression in budding yeast. In the presence of the microtubule-depolymerizing drug benomyl, cells fail to enter the meiotic program and arrest in G_1. When

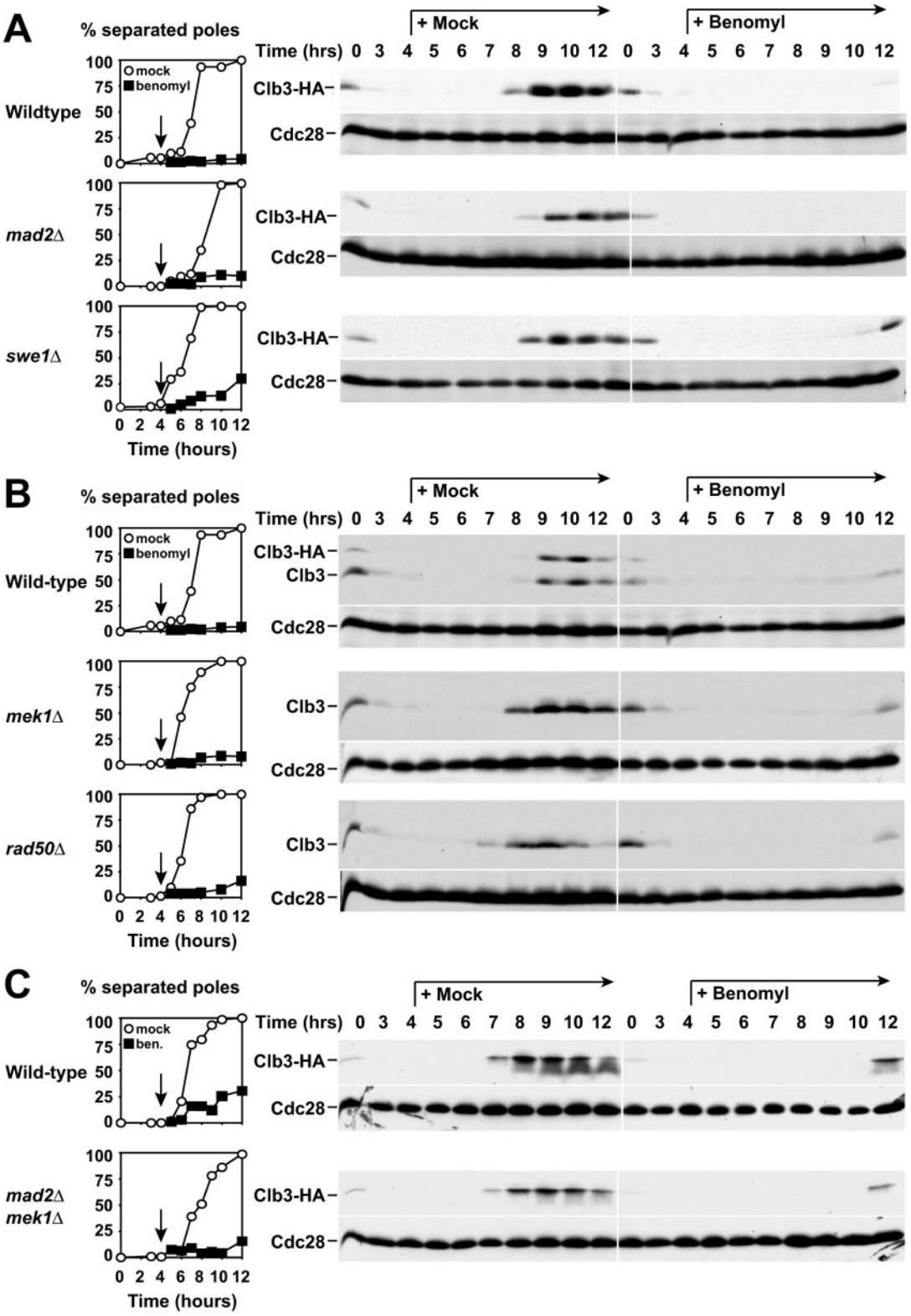

FIG. 8. The benomyl-induced G_2 arrest does not require the spindle checkpoint or the recombination checkpoint. Wild-type (4563), *mad2*Δ (A4843), *swe1*Δ (A4704), *mek1*Δ (A4838), *rad50*Δ (A1771), and *mad2*Δ *mek1*Δ (A12927) cells were studied. At 4 h after induction of meiosis at room temperature (black arrow), cells were resuspended in medium containing 0.4% DMSO (mock; white circles and left panels) or 120 μg/ml benomyl (black squares and right panels). Graphs on the left indicate percentages of cells containing more than one focus of tubulin staining. Western blot analysis was used to monitor Clb3 and Cdc28 (loading control) levels during the same time course. (A and C) A4563, A4843, A4704, and A12927 carry a *CLB3-3HA* fusion. Polyclonal α-Clb3 antibody was used to determine Clb3 levels shown in panel B.

benomyl is added during or after premeiotic S phase, it causes cells to arrest in G_2 with low levels of Clb-CDK activity and incompletely paired chromosomes. Upon microtubule depolymerization, cells respond with a complex change in the pattern of meiotic gene expression that affects both meiosis-specific genes, as well as loci important for both mitotic and meiotic cell cycle progression. In particular, treatment with benomyl or low-temperature stress causes a shutdown of the meiotic transcriptional cascade. Our data further indicate that this transcriptional change is not a general stress response but specific to perturbation of the microtubule cytoskeleton and is likely to be responsible for the cell cycle and developmental arrest. Finally, our results show that the effects of benomyl on meiotic cell cycle progression are not mediated by any known checkpoint pathways pointing to the existence of a novel mechanism responsible for monitoring microtubule integrity and responding to perturbations.

Novel response to microtubule perturbation. It has been reported that treatment of cells with only 60 μg/ml benomyl causes a delay in metaphase I (56). However, at this concentration, cells were still able to segregate their chromosomes, indicating that a transient meiotic spindle could still form (56). When benomyl is added at a concentration of 120 μg/ml, microtubules completely depolymerize. We find that treatment of meiotic cells with such a high dose of benomyl causes a G_1 arrest when it is added during induction of meiosis, or a G_2 arrest when cells are treated during S phase or G_2. Furthermore, the G_2 arrest is accompanied by a dramatic drop in mRNA levels of meiosis-specific genes and meiotically expressed cell cycle regulators. A key question is whether these events are the result of a general stress response or of a specific response mediated by microtubule perturbations. Several lines of evidence indicate that the latter is the case. First, benomyl is a well-characterized microtubule-depolymerizing agent, and the concentration of benomyl used in this study elicits the characteristic metaphase arrest during the mitotic divisions. Second, at least the G_2 arrest caused by benomyl is fully reversible. When the drug is removed, cells progress through meiosis and form viable spores with normal efficiency. Third, cells carrying the *tub2-150* allele, in which microtubules are stabilized and less vulnerable to microtubule-depolymerizing agents (35, 62), are able to enter meiosis and progress through premeiotic S phase in the presence of 120 μg/ml benomyl, indicating that the G_1 arrest caused by benomyl is mediated by the drug's microtubule-depolymerizing function. The transcriptional response observed when benomyl is added 4 h after induction of meiosis is also at least in part mediated by benomyl-induced microtubule perturbations. In *tub2-150* cells, renewed exposure to benomyl 4 h after transfer into meiosis-inducing conditions did cause a drop in RNA levels, but this drop was significantly less dramatic than that observed when wild-type cells are treated in this way. Given that *tub2-150* microtubules still respond to benomyl, some microtubule depolymerization is likely to occur when the cell are reexposed to the drug, which may explain the partial drop in RNA levels that is observed.

A fourth line of evidence indicating that the cell cycle response to benomyl is not a general stress response is that hypertonic stress, a condition not known to affect microtubule structures, fails to cause a cell cycle arrest in G_2 or to down-regulate mRNAs. In contrast, low temperature (14) affects cell cycle progression and genome-wide transcript levels in a manner qualitatively very similar to that of benomyl. We were not able to examine the effects of other fungal microtubule drugs such as thiabendazole, carbendazim, or nocodazole on meiotic cell cycle progression because these drugs are not sufficiently soluble in sporulation medium. However, it is interesting that microtubule-depolymerizing drugs such as colchicine and vinblastine that are structurally quite different from benomyl (11) perturb meiotic prophase in other organisms, such as mice, ciliates, and plants (1, 23, 33, 55, 70). Taken together, these findings indicate that the response of meiotic cells to high levels of benomyl or low temperatures is specific and due to microtubule perturbations.

Benomyl treatment causes a cell cycle arrest in G_1 and G_2. The response of cells to benomyl during entry into the meiotic cell cycle (G_1) and the response during S phase/G_2 appear similar. The G_2 arrest is accompanied by changes in expression levels of several hundred genes. Likewise, transcripts that are affected by benomyl during S phase/G_2, such as *IME2* and *RPL3*, are also down-regulated by benomyl treatment during G_1. We do not know how benomyl causes a cell cycle arrest in G_1 or G_2, but our data indicate that the arrest is a consequence of the fact that it causes microtubules to depolymerize. Cells carrying the *tub2-150* allele enter and progress through premeiotic S phase efficiently even when benomyl is added to the medium. In this context, it is interesting that disruption of microtubule dynamics by inactivating the microtubule motor *KAR3* or its associated factor *CIK1* also causes defects in meiotic entry and a meiotic cell cycle arrest in G_2 (4, 53, 54). It is possible that a similar transcriptional response underlies the meiotic defects of these mutants.

The nature of the cell cycle arrest is also unclear. The G_2 arrest elicited by benomyl is triggered by neither the activation of the spindle assembly nor the recombination checkpoint nor their combined activation. The arrest is also independent of the stress kinase Hog1, since *hog1*Δ cells still arrest in G_2 after benomyl treatment. This suggests that a novel, as-yet-uncharacterized pathway mediates cell cycle arrest in G_2 in response to microtubule perturbations caused by benomyl and low-temperature stress. We do not know much about this response, the factors involved, or the nature of the signal triggering it—possible candidates for signals would be unattached kinetochores or the level of free tubulin dimers. It is clear, however, that one of the consequences of this response is a dramatic change in gene expression. How are these changes in transcription mediated? Obvious targets of the response mechanism to microtubule depolymerization would be transcription factors involved in stress response or mitotic and meiotic gene expression. Meiosis is controlled by a complex transcriptional cascade (25). Induction of early meiotic genes is necessary for the correct expression of the subsequent middle and mid-late meiotic genes. Thus, observed delays in induction of later meiotic genes are likely a consequence of a failure early in the expression cascade. However, the transcriptional decrease also coordinately affects general cell cycle factors including most components of the APC/C and other genes involved in chromosome segregation and cell cycle progression. We therefore favor the idea that the expression and/or activity of a number of mitotic and meiotic transcriptional regulators might be co-

ordinately decreased in response to microtubule depolymerization. Indeed, the meiotic transcription factors *IME1*, *UME6*, *ABF1*, and *NDT80*, as well as the cell cycle regulators *SWI4* and *NDD1*, were expressed at lower levels in response to benomyl, while their transcriptional levels were reestablished when cells began to escape from the arrest. Note that the *IME1* promoter does not appear to respond to temperature stress during early meiosis (Fig. 8D), so the inactivation of the meiotic cascade by cold shock may involve, if Ime1 is affected at all, a posttranslational mechanism. A possible explanation for this orchestrated response of transcription factors to microtubule instability could be auto- and cross-regulation of the factors, which renders them interdependent. It has been suggested that Abf1 and Ndt80 are involved in their own regulation (16, 25, 40). Moreover, Ume6 is required for correct *IME1* and *NDT80* expression (68). Finally, Abf1 may be required for normal *IME1* and *UME6* expression (45). Irrespective of the mechanism eliciting this response, it is clear that that the cell cycle arrest caused by benomyl is a consequence of the transcriptional response, because mRNA levels of factors essential for entry into meiosis I, such as B-type cyclins and the CDK Cdc28, are down-regulated.

Why does microtubule perturbation cause a G_1 or G_2 arrest during the meiotic cell cycle? In mitotically dividing cells, the sole arrest elicited by microtubule depolymerization is a metaphase arrest (22) with no known effects on gene expression (S. Biggins, personal communication). In cells undergoing the meiotic cell cycle, complete microtubule depolymerization causes cells to arrest in G_1 or G_2. Why is the response to benomyl different between these two types of cell cycles? The decision not to enter the meiotic cell cycle when microtubules become unstable may be related to the fact that the meiotic cell cycle occurs under conditions where nutrients are limited. Delays in cell cycle progression caused by perturbations of the microtubule cytoskeleton or any other stresses could thus lead to cell death. Microtubule depolymerization and other stress-sensing mechanisms may therefore be in place during G_1 that prevent entry into the cell cycle when conditions are not favorable for completion of this cell cycle. In this regard, it is interesting that treatment of cells with the DNA replication inhibitor hydroxyurea also inhibits entry into the meiotic cell cycle (10).

The reason why meiotic cells whose microtubules have disassembled arrest in G_2 rather than metaphase I may lie in the way in which the meiotic cell cycle is organized. Once cells have entered meiosis I, cell cycle events are no longer coupled with the developmental program. For example, the monopolin complex, a kinetochore-bound protein complex that promotes the attachment of sister chromatids to microtubules emanating from the same spindle pole (46), dissociates from kinetochores in a manner uncoordinated with other cell cycle events. When cells are arrested in metaphase I through the inactivation of the APC/C activator Cdc20, the developmental program continues. Cdc20-depleted cells initiate spore formation despite arresting with metaphase I spindles (29). Furthermore, the monopolin complex dissociates from kinetochores at the time when it dissociates from wild-type cells despite being arrested in metaphase I (29). Thus, if microtubule depolymerization were to cause cell cycle arrest in metaphase, as it does during the mitotic divisions, the results for meiotic development would be disastrous. During the metaphase I arrest, the monopolin complex would dissociate from kinetochores and upon repolymerization of microtubules, attachment of microtubules to sister kinetochores in a cooriented manner would not occur; hence, meiosis I segregation would fail. In contrast, halting of cells in a cell cycle stage in which the cell cycle is still coordinated with the developmental program would allow cells to resume the meiotic cell cycle upon repolymerization of microtubules and therefore permit the successful completion of the meiotic cell cycle. This is achieved by the arrest in G_2, prior to the commitment to meiosis I. At this stage, both the developmental program and the cell cycle program still rely on the same transcription factor, Ndt80, for their initiation.

Transcriptional changes in response to microtubule depolymerization are not a phenomenon restricted to budding yeast. Changes in RNA levels upon colchicine treatment have been observed in a variety of tissue culture cells (9) and a microtubule-associated transcription factor that activates transcription following microtubule instability has been reported (72). Furthermore, as we observed with budding yeast, several widely divergent organisms, including mouse, *Allium*, and lily, exhibit a meiotic prophase arrest or delay upon exposure to microtubule poisons (33, 55, 60). Indeed, the existence of a prophase "colchicine checkpoint" in mouse spermatocytes has been previously suggested (60, 61). Interestingly, mammalian tissue culture cells show an arrest response to the microtubule drugs colchicine and nocodazole even in mitotic prophase (39, 47). It will be interesting to determine whether these arrests are caused by a transcriptional response similar to that observed in budding yeast.

ACKNOWLEDGMENTS

We are grateful to N. Kleckner and F. Solomon for reagents and advice and to S. Biggins for sharing unpublished results. We thank F. Solomon and members of the Amon lab for their critical reading of the manuscript. We thank L. Hermida for administration of the Germ Online database.

P.D. and G.W. are supported by the Department of Clinical and Biological Sciences and the Biozentrum, respectively. M.C. and C.N.-W. are supported by the Swiss Institute of Bioinformatics. This research was supported by a National Institutes of Health grant (GM62207) to A.A. A.A. is an Investigator of the Howard Hughes Medical Institute.

REFERENCES

1. **Allen, J. W., J. B. Gibson, P. A. Poorman, L. C. Backer, and M. J. Moses.** 1988. Synaptonemal complex damage induced by clastogenic and anti-mitotic chemicals: implications for non-disjunction and aneuploidy. Mutat. Res. **201:**313–324.
2. **Amon, A., M. Tyers, B. Futcher, and K. Nasmyth.** 1993. Mechanisms that help the yeast cell cycle clock tick: G2 cyclins transcriptionally activate G2 cyclins and repress G1 cyclins. Cell **74:**993–1007.
3. **Bailis, J. M., and G. S. Roeder.** 2000. Pachytene exit controlled by reversal of Mek1-dependent phosphorylation. Cell **101:**211–221.
4. **Bascom-Slack, C. A., and D. S. Dawson.** 1997. The yeast motor protein, Kar3p, is essential for meiosis I. J. Cell Biol. **139:**459–467.
5. **Buonomo, S. B., K. P. Rabitsch, J. Fuchs, S. Gruber, M. Sullivan, F. Uhlmann, M. Petronczki, A. Toth, and K. Nasmyth.** 2003. Division of the nucleolus and its release of CDC14 during anaphase of meiosis I depends on separase, SPO12, and SLK19. Dev. Cell **4:**727–739.
6. **Cao, L., E. Alani, and N. Kleckner.** 1990. A pathway for generation and processing of double-strand breaks during meiotic recombination in S. cerevisiae. Cell **61:**1089–1101.
7. **Chu, S., J. DeRisi, M. Eisen, J. Mulholland, D. Botstein, P. O. Brown, and I. Herskowitz.** 1998. The transcriptional program of sporulation in budding yeast. Science **282:**699–705.
8. **Chu, S., and I. Herskowitz.** 1998. Gametogenesis in yeast is regulated by a transcriptional cascade dependent on Ndt80. Mol. Cell **1:**685–696.

9. **Cleveland, D. W., M. A. Lopata, P. Sherline, and M. W. Kirschner.** 1981. Unpolymerized tubulin modulates the level of tubulin mRNAs. Cell **25:**537–546.
10. **Davis, L., M. Barbera, A. McDonnell, K. McIntyre, R. Sternglanz, Q. Jin, J. Loidl, and J. Engebrecht.** 2001. The Saccharomyces cerevisiae MUM2 gene interacts with the DNA replication machinery and is required for meiotic levels of double strand breaks. Genetics **157:**1179–1189.
11. **Downing, K. H.** 2000. Structural basis for the interaction of tubulin with proteins and drugs that affect microtubule dynamics. Annu. Rev. Cell Dev. Biol. **16:**89–111.
12. **Edgar, R., M. Domrachev, and A. E. Lash.** 2002. Gene expression omnibus: NCBI gene expression and hybridization array data repository. Nucleic Acids Res. **30:**207–210.
13. **Giaever, G., A. M. Chu, L. Ni, C. Connelly, L. Riles, S. Veronneau, S. Dow, A. Lucau-Danila, K. Anderson, B. Andre, A. P. Arkin, A. Astromoff, M. El-Bakkoury, R. Bangham, R. Benito, S. Brachat, S. Campanaro, M. Curtiss, K. Davis, A. Deutschbauer, K. D. Entian, P. Flaherty, F. Foury, D. J. Garfinkel, M. Gerstein, D. Gotte, U. Guldener, J. H. Hegemann, S. Hempel, Z. Herman, D. F. Jaramillo, D. E. Kelly, S. L. Kelly, P. Kotter, D. LaBonte, D. C. Lamb, N. Lan, H. Liang, H. Liao, L. Liu, C. Luo, M. Lussier, R. Mao, P. Menard, S. L. Ooi, J. L. Revuelta, C. J. Roberts, M. Rose, P. Ross-Macdonald, B. Scherens, G. Schimmack, B. Shafer, D. D. Shoemaker, S. Sookhai-Mahadeo, R. K. Storms, J. N. Strathern, G. Valle, M. Voet, G. Volckaert, C. Y. Wang, T. R. Ward, J. Wilhelmy, E. A. Winzeler, Y. Yang, G. Yen, E. Youngman, K. Yu, H. Bussey, J. D. Boeke, M. Snyder, P. Philippsen, R. W. Davis, and M. Johnston.** 2002. Functional profiling of the Saccharomyces cerevisiae genome. Nature **418:**387–391.
14. **Gupta, M. L., Jr., C. J. Bode, C. A. Dougherty, R. T. Marquez, and R. H. Himes.** 2001. Mutagenesis of beta-tubulin cysteine residues in Saccharomyces cerevisiae: mutation of cysteine 354 results in cold-stable microtubules. Cell Motil. Cytoskeleton **49:**67–77.
15. **Guttmann-Raviv, N., S. Martin, and Y. Kassir.** 2002. Ime2, a meiosis-specific kinase in yeast, is required for destabilization of its transcriptional activator, Ime1. Mol. Cell. Biol. **22:**2047–2056.

15a. **Harris, M. A., J. Clark, A. Ireland, J. Lomax, M. Ashburner, R. Foulger, K. Eilbeck, S. Lewis, B. Marshall, C. Mungall, J. Richter, G. M. Rubin, J. A. Blake, C. Bult, M. Dolan, H. Drabkin, J. T. Eppig, D. P. Hill, L. Ni, M. Ringwald, R. Balakrishnan, J. M. Cherry, K. R. Christie, M. C. Costanzo, S. S. Dwight, S. Engel, D. G. Fisk, J. E. Hirschman, E. L. Hong, R. S. Nash, A. Sethuraman, C. L. Theesfeld, D. Botstein, K. Dolinski, B. Feierbach, T. Berardini, S. Mundodi, S. Y. Rhee, R. Apweiler, D. Barrell, E. Camon, E. Dimmer, V. Lee, R. Chisholm, P. Gaudet, W. Kibbe, R. Kishore, E. M. Schwarz, P. Sternberg, M. Gwinn, L. Hannick, J. Wortman, M. Berriman, V. Wood, N. de la Cruz, P. Tonellato, P. Jaiswal, T. Seigfried, and R. White.** 2004. The Gene Ontology (GO) database and informatics resource. Nucleic Acids Res. **32:**D258–D261.

16. **Hepworth, S. R., H. Friesen, and J. Segall.** 1998. NDT80 and the meiotic recombination checkpoint regulate expression of middle sporulation-specific genes in *Saccharomyces cerevisiae*. Mol. Cell. Biol. **18:**5750–5761.
17. **Honigberg, S. M., and K. Purnapatre.** 2003. Signal pathway integration in the switch from the mitotic cell cycle to meiosis in yeast. J. Cell Sci. **116:**2137–2147.
18. **Hosack, D. A., G. Dennis, Jr., B. T. Sherman, H. C. Lane, and R. A. Lempicki.** 2003. Identifying biological themes within lists of genes with EASE. Genome Biol. **4:**R70.
19. **Huber, W., A. von Heydebreck, H. Sultmann, A. Poustka, and M. Vingron.** 2002. Variance stabilization applied to microarray data calibration and to the quantification of differential expression. Bioinformatics **18**(Suppl. 1)**:**S96–S104.
20. **Hwang, L. H., L. F. Lau, D. L. Smith, C. A. Mistrot, K. G. Hardwick, E. S. Hwang, A. Amon, and A. W. Murray.** 1998. Budding yeast Cdc20: a target of the spindle checkpoint. Science **279:**1041–1044.
21. **Irizarry, R. A., B. M. Bolstad, F. Collin, L. M. Cope, B. Hobbs, and T. P. Speed.** 2003. Summaries of Affymetrix GeneChip probe level data. Nucleic Acids Res. **31:**e15.
22. **Jacobs, C. W., A. E. Adams, P. J. Szaniszlo, and J. R. Pringle.** 1988. Functions of microtubules in the Saccharomyces cerevisiae cell cycle. J. Cell Biol. **107:**1409–1426.
23. **Kaczanowski, A., J. Gaertig, and J. Kubiak.** 1985. Effect of the antitubulin drug nocodazole on meiosis and postmeiotic development in Tetrahymena thermophila. Induction of achiasmatic meiosis. Exp. Cell Res. **158:**244–256.
24. **Kane, S. M., and R. Roth.** 1974. Carbohydrate metabolism during ascospore development in yeast. J. Bacteriol. **118:**8–14.
25. **Kassir, Y., N. Adir, E. Boger-Nadjar, N. G. Raviv, I. Rubin-Bejerano, S. Sagee, and G. Shenhar.** 2003. Transcriptional regulation of meiosis in budding yeast. Int. Rev. Cytol. **224:**111–171.
26. **Kaufman, L., and P. J. Rousseeuw.** 1987. Clustering by means of mediods, p. 405–416. *In* Y. Dodge (ed.), Statistical data analysis based on the L1-norm and related methods. North-Holland/Elsevier, Amsterdam, The Netherlands.
27. **Klein, F., P. Mahr, M. Galova, S. B. C. Buonomo, C. Michaelis, K. Nairz, and K. Nasmyth.** 1999. A central role for cohesins in sister chromatid cohesion, formation of axial elements and recombination during yeast meiosis. Cell **98:**91–103.
28. **Kohrer, K., and H. Domdey.** 1991. Preparation of high molecular weight RNA. Methods Enzymol. **194:**398–405.
29. **Lee, B. H., and A. Amon.** 2003. Role of Polo-like kinase CDC5 in programming meiosis I chromosome segregation. Science **300:**482–486.
30. **Leisch, F.** 2002. Sweave: dynamic generation of statistical reports using literate data analysis, p. 575–580. *In* W. Hardle and B. Ronz (ed.), Compstat 2002—proceedings in computational statistics. Physika Verlag, Heidelberg, Germany.
31. **Leu, J. Y., and G. S. Roeder.** 1999. The pachytene checkpoint in S. cerevisiae depends on Swe1-mediated phosphorylation of the cyclin-dependent kinase Cdc28. Mol. Cell **4:**805–814.
32. **Lew, D. J., and D. J. Burke.** 2003. The spindle assembly and spindle position checkpoints. Annu. Rev. Genet. **37:**251–282.
33. **Loidl, J.** 1988. The effect of colchicine on synaptonemal complex formation in Allium ursinum. Exp. Cell Res. **178:**93–97.
34. **Longtine, M. S., A. McKenzie III, D. J. Demarini, N. G. Shah, A. Wach, A. Brachat, P. Philippsen, and J. R. Pringle.** 1998. Additional modules for versatile and economical PCR-based gene deletion and modification in Saccharomyces cerevisiae. Yeast **14:**953–961.
35. **Machin, N. A., J. M. Lee, and G. Barnes.** 1995. Microtubule stability in budding yeast: characterization and dosage suppression of a benomyl-dependent tubulin mutant. Mol. Biol. Cell **6:**1241–1259.
36. **Marston, A. L., B. H. Lee, and A. Amon.** 2003. The Cdc14 phosphatase and the FEAR network control meiotic spindle disassembly and chromosome segregation. Dev. Cell **4:**711–726.
37. **Marston, A. L., W. H. Tham, H. Shah, and A. Amon.** 2004. A genome-wide screen identifies genes required for centromeric cohesion. Science **303:**1367–1370.
38. **Michaelis, C., R. Ciosk, and K. Nasmyth.** 1997. Cohesins: chromosomal proteins that prevent premature separation of sister chromatids. Cell **91:**35–45.
39. **Mikhailov, A., and C. L. Rieder.** 2002. Cell cycle: stressed out of mitosis. Curr. Biol. **12:**R331–R333.
40. **Miyake, T., J. Reese, C. M. Loch, D. T. Auble, and R. Li.** 2004. Genome-wide analysis of ARS (autonomously replicating sequence) binding factor 1 (Abf1p)-mediated transcriptional regulation in Saccharomyces cerevisiae. J. Biol. Chem. **279:**34865–34872.
41. **Morgan, D. O.** 1997. Cyclin-dependent kinases: engines, clocks, and microprocessors. Annu. Rev. Cell Dev Biol. **13:**261–291.
42. **Nairz, K., and F. Klein.** 1997. mre11S—a yeast mutation that blocks double-strand-break processing and permits nonhomologous synapsis in meiosis. Genes Dev. **11:**2272–2290.
43. **Primig, M., C. Wiederkehr, R. Basavaraj, C. Sarrauste de Menthiere, L. Hermida, R. Koch, U. Schlecht, H. G. Dickinson, M. Fellous, J. A. Grootegoed, R. S. Hawley, B. Jegou, B. Maro, A. Nicolas, T. Orr-Weaver, T. Schedl, A. Villeneuve, D. J. Wolgemuth, M. Yamamoto, D. Zickler, N. Lamb, and R. E. Esposito.** 2003. GermOnline, a new cross-species community annotation database on germ-line development and gametogenesis. Nat. Genet. **35:**291–292.
44. **Primig, M., R. M. Williams, E. A. Winzeler, G. G. Tevzadze, A. R. Conway, S. Y. Hwang, R. W. Davis, and R. E. Esposito.** 2000. The core meiotic transcriptome in budding yeasts. Nat. Genet. **26:**415–423.
45. **Prinz, S., F. Klein, H. Auer, D. Schweizer, and M. Primig.** 1995. A DNA binding factor (UBF) interacts with a positive regulatory element in the promoters of genes expressed during meiosis and vegetative growth in yeast. Nucleic Acids Res. **23:**3449–3456.
46. **Rabitsch, K. P., M. Petronczki, J. P. Javerzat, S. Genier, B. Chwalla, A. Schleiffer, T. U. Tanaka, and K. Nasmyth.** 2003. Kinetochore recruitment of two nucleolar proteins is required for homolog segregation in meiosis I. Dev. Cell **4:**535–548.
47. **Rieder, C. L., and R. Cole.** 2000. Microtubule disassembly delays the G2-M transition in vertebrates. Curr. Biol. **10:**1067–1070.
48. **Roeder, G. S.** 1997. Meiotic chromosomes: it takes two to tango. Genes Dev. **11:**2600–2621.
49. **Roeder, G. S., and J. M. Bailis.** 2000. The pachytene checkpoint. Trends Genet. **16:**395–403.
50. **Saunders, W., D. Hornack, V. Lengyel, and C. Deng.** 1997. The Saccharomyces cerevisiae kinesin-related motor Kar3p acts at preanaphase spindle poles to limit the number and length of cytoplasmic microtubules. J. Cell Biol. **137:**417–431.
51. **Schlecht, U., P. Demougin, R. Koch, L. Hermida, C. Wiederkehr, P. Descombes, C. Pineau, B. Jegou, and M. Primig.** 2004. Expression profiling of mammalian male meiosis and gametogenesis identifies novel candidate genes for roles in the regulation of fertility. Mol. Biol. Cell **15:**1031–1043.
52. **Schlecht, U., and M. Primig.** 2003. Mining meiosis and gametogenesis with DNA microarrays. Reproduction **125:**447–456.
53. **Shanks, R. M., C. Bascom-Slack, and D. S. Dawson.** 2004. Analysis of the kar3 meiotic arrest in Saccharomyces cerevisiae. Cell Cycle **3:**363–371.
54. **Shanks, R. M., R. J. Kamieniecki, and D. S. Dawson.** 2001. The Kar3-

interacting protein Cik1p plays a critical role in passage through meiosis I in Saccharomyces cerevisiae. Genetics **159:**939–951.

55. **Shepard, J., E. R. Boothroyd, and H. Stern.** 1974. The effect of colchicine on synapsis and chiasma formation in microsporocytes of *Lilium.* Chromosoma **44:**423–437.
56. **Shonn, M. A., R. McCarroll, and A. W. Murray.** 2000. Requirement of the spindle checkpoint for proper chromosome segregation in budding yeast meiosis. Science **289:**300–303.
57. **Shonn, M. A., A. L. Murray, and A. W. Murray.** 2003. Spindle checkpoint component Mad2 contributes to biorientation of homologous chromosomes. Curr. Biol. **13:**1979–1984.
58. **Sora, S., P. Melchioretto, P. Primignani, and M. L. Agostoni Carbone.** 1988. Caffeine interactions with methyl methanesulphonate, hycanthone, benlate, and cadmium chloride in chromosomal meiotic segregation of Saccharomyces cerevisiae. Mutat. Res. **201:**9–16.
59. **Sym, M., J. A. Engebrecht, and G. S. Roeder.** 1993. ZIP1 is a synaptonemal complex protein required for meiotic chromosome synapsis. Cell **72:**365–378.
60. **Tepperberg, J. H., M. J. Moses, and J. Nath.** 1997. Colchicine effects on meiosis in the male mouse. I. Meiotic prophase: synaptic arrest, univalents, loss of damaged spermatocytes and a possible checkpoint at pachytene. Chromosoma **106:**183–192.
61. **Tepperberg, J. H., M. J. Moses, and J. Nath.** 1999. Colchicine effects on meiosis in the male mouse. II. Inhibition of synapsis and induction of nondisjunction. Mutat. Res. **429:**93–105.
62. **Thomas, J. H., N. F. Neff, and D. Botstein.** 1985. Isolation and characterization of mutations in the beta-tubulin gene of Saccharomyces cerevisiae. Genetics **111:**715–734.
63. **Tung, K. S., E. J. Hong, and G. S. Roeder.** 2000. The pachytene checkpoint prevents accumulation and phosphorylation of the meiosis-specific transcription factor Ndt80. Proc. Natl. Acad. Sci. USA **97:**12187–12192.
64. **Visintin, R., K. Craig, E. S. Hwang, S. Prinz, M. Tyers, and A. Amon.** 1998. The phosphatase Cdc14 triggers mitotic exit by reversal of Cdk-dependent phosphorylation. Mol. Cell **2:**709–718.
65. **Visintin, R., E. S. Hwang, and A. Amon.** 1999. Cfi1 prevents premature exit from mitosis by anchoring Cdc14 phosphatase in the nucleolus. Nature **398:**818–823.
66. **Wiederkehr, C., R. Basavaraj, C. Sarrauste de Menthiere, L. Hermida, R. Koch, U. Schlecht, A. Amon, S. Brachat, M. Breitenbach, P. Briza, S. Caburet, M. Cherry, R. Davis, A. Deutschbauer, H. G. Dickinson, T. Dumitrescu, M. Fellous, A. Goldman, J. A. Grootegoed, R. Hawley, R. Ishii, B. Jegou, R. J. Kaufman, F. Klein, N. Lamb, B. Maro, K. Nasmyth, A. Nicolas, T. Orr-Weaver, P. Philippsen, C. Pineau, K. P. Rabitsch, V. Reinke, H. Roest, W. Saunders, M. Schroder, T. Schedl, M. Siep, A. Villeneuve, D. J. Wolgemuth, M. Yamamoto, D. Zickler, R. E. Esposito, and M. Primig.** 2004. GermOnline, a cross-species community knowledgebase on germ cell differentiation. Nucleic Acids Res. **32:**D560–D567.
67. **Wiederkehr, C., R. Basavaraj, C. Sarrauste de Menthiere, R. Koch, U. Schlecht, L. Hermida, B. Masdoua, R. Ishii, V. Cassen, M. Yamamoto, C. Lane, M. Cherry, N. Lamb, and M. Primig.** 2004. Database model and specification of GermOnline Release 2.0, a cross-species community annotation knowledgebase on germ cell differentiation. Bioinformatics **20:**808–811.
68. **Williams, R. M., M. Primig, B. K. Washburn, E. A. Winzeler, M. Bellis, C. Sarrauste de Menthiere, R. W. Davis, and R. E. Esposito.** 2002. The Ume6 regulon coordinates metabolic and meiotic gene expression in yeast. Proc. Natl. Acad. Sci. USA **99:**13431–13436.
69. **Xu, L., B. M. Weiner, and N. Kleckner.** 1997. Meiotic cells monitor the status of the interhomolog recombination complex. Genes Dev. **11:**106–118.
70. **Zickler, D., and N. Kleckner.** 1998. The leptotene-zygotene transition of meiosis. Annu. Rev. Genet. **32:**619–697.
71. **Zickler, D., and N. Kleckner.** 1999. Meiotic Chromosomes: integrating structure and function. Annu. Rev. Genet. **33:**603–754.
72. **Ziegelbauer, J., B. Shan, D. Yager, C. Larabell, B. Hoffmann, and R. Tjian.** 2001. Transcription factor MIZ-1 is regulated via microtubule association. Mol. Cell **8:**339–349.